Zircon U–Pb geochronology and geochemistry of rhyolitic tuff, granite porphyry and syenogranite in the Lengshuikeng ore district, SE China: Implications for a continental arc to intra-arc rift setting

Changming Wang[1,*], Da Zhang[2], Ganguo Wu[1], Yigan Xu[1], Emmanuel John M Carranza[3], Yaoyao Zhang[1], Huaikun Li[4] and Jianzhen Geng[4]

[1]*State Key Laboratory of Geological Processes and Mineral Resources, China University of Geosciences, Beijing 100083, China.*
[2]*No. 912 Geological Surveying Team, Bureau of Geology and Mineral Exploration and Development, Yingtan 334000, China.*
[3]*Geo-Information Science and Earth Observation (ITC), University of Twente, Enschede, The Netherlands.*
[4]*Tianjin Center of China Geological Survey, Tianjin 300170, China.*
[*]*Corresponding author. e-mail: wangcm@cugb.edu.cn*

SE China is well known for its Mesozoic large-scale granitoid plutons and associated ore deposits. Here, zircon U–Pb geochronological and geochemical data have been used to better constrain the petrogenesis of the igneous rocks associated with porphyry Ag–Pb–Zn deposits in the Lengshuikeng ore district, SE China. The Lengshuikeng rhyolitic tuff, granite porphyry and syenogranite yielded zircon U–Pb ages of 161, 155 and 138 Ma, respectively. The Lengshuikeng granite porphyries belong to calc-alkaline series and show fractionated I-type affinities. The rhyolitic tuffs show almost similar characteristics as the granite porphyries. The Lengshuikeng syenogranites are all alkali-rich and show A-type affinities. The syenogranites have high contents of high field strength elements such as Nb, Ta, Zr, Hf; with Zr + Nb + Ce + Y contents of >350 ppm. Chondrite-normalized REE patterns show relative enrichment of LREEs and strong negative Eu anomalies. The Lengshuikeng granite porphyries, syenogranites and tuffs were probably derived from partial melting of underlying Proterozoic metasedimentary rocks with minor addition of mantle-derived magmas, accompanied by fractional crystallization. Detailed petrologic and geochemical data for the Jurassic igneous rocks from the Lengshuikeng ore district imply that during the Late Jurassic, SE China on the southeast of the Shi-Hang zone was a continental arc associated with the subduction of the Palaeo-Pacific plate and that since the beginning of the Early Cretaceous an intra-arc rift has been formed along the Shi-Hang zone.

1. Introduction

Over past several decades, research on porphyry types of mineral deposits in SE China was focused on the Yangtze Block (e.g., the Fujiawu, Zhushahong and Tongchang deposits in the Dexing ore field, and the Tongshankou, Chengmenshan, Fengshandong, Shaxi and Anjishan deposits in the

Keywords. A-type; I-type; continental arc; rifting; Lengshuikeng; southeast China.

J. Earth Syst. Sci. **122**, No. 3, June 2013, pp. 809–830

Lower Yangtze River metallogenic belt). All of the above-mentioned deposits are related to the Late Mesozoic (Yanshanian) magmatism marked by abundant granitoids and volcanic rocks in SE China (Li 2000; Li and Li 2007; Li *et al.* 2007). The proposed geodynamic settings and tectonic regimes of these magmatic rocks remain enigmatic, such as the Alpine-type collision between

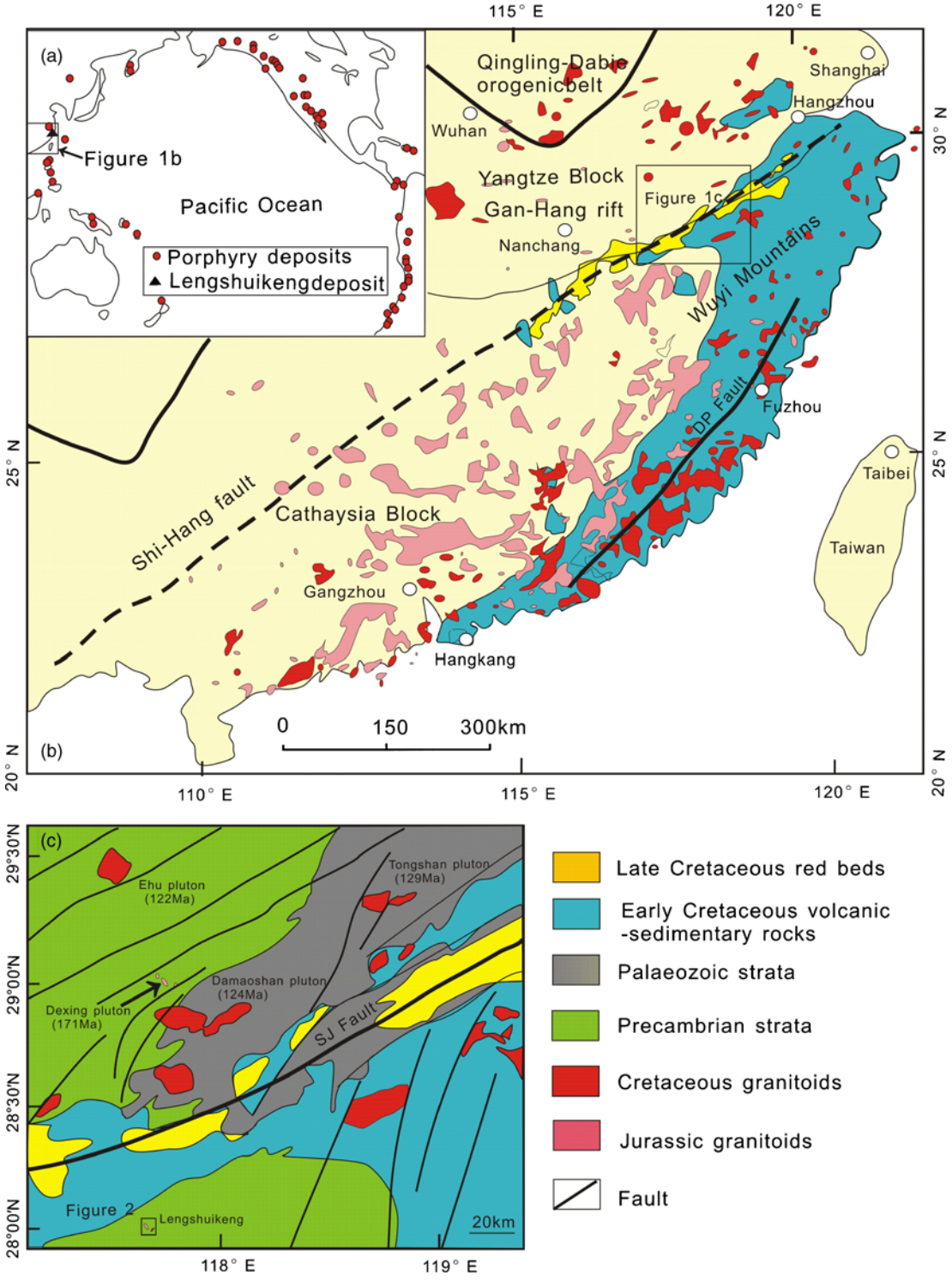

Figure 1. Sketch map showing (**a**) the circum-Pacific porphyry copper ore belt (modified after Jiang *et al.* 2011); (**b**) the late Mesozoic volcanic-intrusive complex belt in SE China (modified after Jiang *et al.* 2011); and (**c**) the regional geology of the Lengshuikeng ore district (modified after Wang *et al.* 2011). Major faults in study area: Qin–Hang, Qinzhou–Hangzhou as collision-induced suture zone between the Cathaysian and the Yangtze blocks; SJ: Shaoxing–Jiangshan; ZD: Zhenghe–Dapu.

the Yangtze and Cathaysia Blocks (Hsü *et al.* 1990; Gilder *et al.* 1991), continental rifting and basin formation (Jahn *et al.* 1990; Li 2000), and the active continental margin model related to the subduction of the Palaeo-Pacific plate (Charvet *et al.* 1994a, b; Martin *et al.* 1994; Lan *et al.* 1996; Lapierre *et al.* 1997).

The Lengshuikeng ore district, situated in the circum-Pacific porphyry-Cu ore belt (figure 1a), has a reserve of 43 Mt ore with 2.3–7.0% Pb + Zn (or a reserve of ca. 3.9 Mt Pb + Zn) and 204.53 g/t Ag (or a reserve of 9800t Ag). Together with Ag, Pb and Zn, there are other accessory metals, including Cd (13 Kt ore with 0.01% Cd), Au (10.8 t ore with 0.08 g/t Au), S (3.7 Mt ore with 2.47% S) and Fe + Mn (3.9 Mt ore with 24% Fe + Mn) (NGST 1997; Wang *et al.* 2011). Over the past several decades of years, researches in the Lengshuikeng ore district mainly focused on its geological characteristics (Deng 1991; Liu and Shen 1991; Luo 1991; Yao 2003), mineralization and wall rock alteration (Wei 1997), fluid inclusions (Zuo *et al.* 2008) and geochemistry (Chen and Qiu 1995; Chen and Zhou 1988; Xu *et al.* 2001) of the porphyry type Ag–Pb–Zn deposits. Recently, strata-bound Ag–Pb–Zn mineralizations have been found along the periphery and beneath the porphyry type deposits. The stratabound mineralizations are hosted in volcano–sedimentary rocks, which formed during intermittent volcanism in the Upper Jurassic Daguding and E'huling formations. This geological setting and associated mineral assemblages are quite unique for porphyry-type deposits, and therefore are worthy of detailed research (e.g., Meng *et al.* 2007; Wang *et al.* 2011).

Although the geochronology of host rocks in the Lengshuikeng ore district has been the focus of many previous studies, the ages of volcanic and intrusive rocks in the district remains controversial, owing to the various dating methods that have been applied, such as the SHRIMP U–Pb, K–Ar, ^{39}Ar–^{40}Ar and Rb–Sr whole-rock isochron methods (e.g., NGST 1997, 2003; Meng *et al.* 2007). However, these methods yield age results that are complicated and inconsistent. For example, the ages of the Lengshuikeng granitic porphyries have been reported as sericite K–Ar ages of 121–138 Ma (NGST 1997), K-feldspar K–Ar age of 136.5 Ma (NGST 1997), whole-rock Rb–Sr age of 159 Ma (Meng *et al.* 2007) and SHRIMP U–Pb age of 162.0 ± 2 Ma (Zuo *et al.* 2010). In order to better constrain the timing of igneous activity in the Lengshuikeng ore district, we carried out zircon U–Pb dating for the rhyolitic tuff, granite porphyry and syenogranite using laser ablation multicollector inductively coupled plasma mass spectrometry (LA-MC-ICP-MS). We also carried out a whole-rock geochemical study in order to constrain the genesis and geodynamic setting of the volcanic and intrusive rocks in Lengshuikeng ore district. Therefore, this paper contributes not only for understanding the genesis and geodynamic setting of Lengshuikeng ore district but also understanding of the large-scale Mesozoic igneous event in SE China.

2. Regional and ore district geology

2.1 *Location and regional geological evolution*

The Lengshuikeng ore district is located in the northern part of the Wuyi Mountains and on the southern side of the Shaoxing–Jiangshan (SJ) fault (Yu *et al.* 2006; Wang *et al.* 2007; Hsieh *et al.* 2008; Charvet *et al.* 2010). This fault is the eastern part of Shiwandashan–Hangzhou (Shi–Hang) fault zone, as a collision-induced suture zone between the Cathaysian and the Yangtze blocks in SE China (figure 1b; Liu *et al.* 2010; Li *et al.* 2011; Wong *et al.* 2011). Collisional amalgamation of the Cathaysian and Yangtze blocks into the so-called 'South China' Block (SCB) began in the early Qingbaikou period (∼950 ± 50 Ma) (Li *et al.* 2008; Wang *et al.* 2008; Chen *et al.* 2009) and was completed by the end of the Jinning orogeny at ca. 850 Ma (Chen *et al.* 1991; Shu *et al.* 1994).

In the Caledonian period (600–405 Ma), the previously amalgamated Yangtze and Cathaysia blocks, which had been rifted apart during the Sinian (ca. 850–600 Ma), collided for a second time and re-established the SCB (Wang *et al.* 2010b, c; Zhou *et al.* 2002). During the Variscan period (405–270 Ma), extension within the SCB resulted in Paleozoic intracontinental rifts. Indosinian collision between the South China and North China blocks began in the Late Palaeozoic and was over in the Late Triassic (ca. 270–208 Ma). A magmatic gap from 208 to 180 Ma characterized the South China block in post-Indosinian time. From Late Triassic to Early Jurassic (180–145 Ma), most areas of the Wuyi mountains were folded and uplifted before undergoing extensional collapse. Subsequently, the region experienced Early Cretaceous granitic magmatism (145–100 Ma) (Deng *et al.* 2009a, 2010, 2011c) and the formation of large-scale Late Cretaceous–Paleogene red bed sedimentary basins between 100 and 70 Ma (Deng *et al.* 2009b, 2011a, b).

2.2 *Stratigraphy*

The stratigraphic sequence in the Lengshuikeng ore district is summarized in table 1 (Wang *et al.*

Table 1. *LA-MC-ICP-MS zircon U–Pb analytical results for the granite porphyry, rhyolitic tuff, and syenogranite in the Lengshuikeng ore district.*

	Content (ppm)		Ratios										Age (Ma)	
Spot number	Pb	U	$^{207}Pb/^{206}Pb$	1σ	$^{207}Pb/^{235}U$	1σ	$^{206}Pb/^{238}U$	1σ	$^{208}Pb/^{232}Th$	1σ	$^{232}Th/^{238}U$	1σ	$^{206}Pb/^{238}U$	1σ
T3.1	3	78	0.0494	0.0080	0.1779	0.0292	0.0261	0.0005	0.0082	0.0002	1.62	0.0079	161	3
T3.2	10	355	0.0504	0.0021	0.1804	0.0077	0.0259	0.0001	0.0076	0.0001	0.89	0.0081	161	1
T3.3	3	88	0.0470	0.0078	0.1699	0.0279	0.0256	0.0004	0.0072	0.0001	2.10	0.0202	161	3
T3.4	10	321	0.0523	0.0025	0.1885	0.0091	0.0262	0.0002	0.0077	0.0001	1.00	0.0055	162	1
T3.5	4	127	0.0529	0.0054	0.1799	0.0185	0.0248	0.0003	0.0074	0.0001	1.66	0.0194	163	2
T3.6	15	435	0.0506	0.0018	0.1762	0.0064	0.0252	0.0001	0.0073	0.0000	1.72	0.0204	159	1
T3.7	7	247	0.0528	0.0026	0.1866	0.0094	0.0256	0.0002	0.0074	0.0001	1.04	0.0039	164	1
T3.8	3	80	0.0455	0.0092	0.1730	0.0351	0.0259	0.0005	0.0074	0.0002	1.75	0.0120	161	3
T3.9	3	96	0.0523	0.0069	0.1813	0.0245	0.0251	0.0004	0.0072	0.0002	1.50	0.0068	163	3
T3.10	4	109	0.0479	0.0072	0.1704	0.0249	0.0252	0.0003	0.0075	0.0001	1.44	0.0056	158	2
T3.11	3	88	0.0476	0.0065	0.1724	0.0227	0.0257	0.0004	0.0076	0.0001	2.41	0.0197	162	3
T3.12	8	264	0.0534	0.0026	0.1851	0.0092	0.0251	0.0002	0.0076	0.0001	1.34	0.0078	161	1
T3.14	5	172	0.0462	0.0045	0.1649	0.0162	0.0258	0.0003	0.0077	0.0002	1.11	0.0128	162	2
T3.15	3	93	0.0506	0.0068	0.1748	0.0232	0.0248	0.0005	0.0074	0.0001	2.01	0.0100	159	3
T3.16	4	133	0.0578	0.0066	0.2006	0.0229	0.0249	0.0004	0.0079	0.0003	0.86	0.0169	164	2
T3.17	7	227	0.0468	0.0030	0.1602	0.0102	0.0248	0.0002	0.0076	0.0001	1.28	0.0080	158	2
T3.18	10	343	0.0511	0.0019	0.1805	0.0070	0.0255	0.0001	0.0080	0.0001	0.79	0.0037	161	1
T3.20	6	174	0.0527	0.0043	0.1784	0.0145	0.0245	0.0002	0.0075	0.0001	1.64	0.0112	157	2
T1.1	8	241	0.0515	0.0028	0.1766	0.0098	0.0248	0.0002	0.0075	0.0001	1.57	0.0153	157	1
T1.2	6	205	0.0478	0.0035	0.1595	0.0118	0.0241	0.0003	0.0074	0.0001	1.40	0.0130	153	1
T1.4	6	198	0.0481	0.0034	0.1637	0.0118	0.0247	0.0002	0.0075	0.0001	0.98	0.0197	157	1
T1.5	2	71	0.0492	0.0090	0.1708	0.0308	0.0252	0.0006	0.0068	0.0002	1.45	0.0059	160	4
T1.7	12	439	0.0483	0.0015	0.1661	0.0050	0.0249	0.0002	0.0073	0.0001	0.74	0.0051	155	1
T1.9	6	143	0.0506	0.0034	0.2515	0.0169	0.0359	0.0003	0.0106	0.0001	1.32	0.0090	227	3
T1.10	2	62	0.0500	0.0116	0.1746	0.0405	0.0253	0.0007	0.0079	0.0002	1.56	0.0142	159	4

T1.11	3	76	0.0473	0.0126	0.1707	0.0427	0.0250	0.0006	0.0077	0.0002	1.97	0.0140	156	4
T1.12	3	79	0.0514	0.0085	0.1731	0.0288	0.0244	0.0005	0.0082	0.0002	1.62	0.0063	155	3
T1.13	5	134	0.0520	0.0056	0.1740	0.0188	0.0240	0.0003	0.0073	0.0001	1.95	0.0079	154	2
T1.14	20	691	0.0476	0.0012	0.1536	0.0038	0.0234	0.0001	0.0071	0.0000	1.21	0.0167	152	1
T1.15	3	105	0.0523	0.0079	0.1715	0.0275	0.0238	0.0006	0.0075	0.0002	1.47	0.0065	154	4
T1.16	3	84	0.0513	0.0075	0.1727	0.0248	0.0241	0.0005	0.0073	0.0002	1.52	0.0065	156	3
T1.18	4	123	0.0506	0.0050	0.1693	0.0169	0.0243	0.0003	0.0073	0.0001	1.69	0.0211	155	2
T1.19	11	376	0.0531	0.0018	0.1800	0.0061	0.0246	0.0001	0.0074	0.0001	0.92	0.0049	156	1
T1.22	3	102	0.0492	0.0081	0.1731	0.0290	0.0255	0.0004	0.0085	0.0002	1.49	0.0058	160	3
T1.23	4	144	0.0492	0.0041	0.1720	0.0147	0.0251	0.0003	0.0075	0.0001	0.83	0.0034	157	2
T1.24	2	80	0.0477	0.0123	0.1630	0.0415	0.0237	0.0007	0.0088	0.0003	1.07	0.0104	154	4
T1.25	11	365	0.0472	0.0019	0.1607	0.0066	0.0246	0.0002	0.0078	0.0001	1.08	0.0043	156	1
T1.26	10	350	0.0501	0.0020	0.1728	0.0072	0.0250	0.0002	0.0089	0.0001	0.89	0.0042	153	1
T13.1	6	223	0.0427	0.0034	0.1286	0.0100	0.0218	0.0001	0.0061	0.0003	1.17	0.0016	139	1
T13.2	13	434	0.0489	0.0010	0.1439	0.0032	0.0214	0.0001	0.0084	0.0004	1.40	0.0007	136	1
T13.3	4	164	0.0489	0.0034	0.1459	0.0102	0.0216	0.0001	0.0066	0.0003	0.98	0.0034	138	1
T13.4	12	442	0.0483	0.0014	0.1444	0.0041	0.0217	0.0001	0.0067	0.0003	1.24	0.0012	138	1
T13.5	4	116	0.0457	0.0043	0.1605	0.0150	0.0255	0.0002	0.0077	0.0004	1.92	0.0023	162	1
T13.6	7	245	0.0485	0.0025	0.1455	0.0076	0.0217	0.0001	0.0068	0.0003	1.53	0.0015	139	1
T13.7	7	244	0.0488	0.0028	0.1476	0.0086	0.0219	0.0001	0.0065	0.0003	1.51	0.0013	140	1
T13.8	5	175	0.0486	0.0038	0.1459	0.0114	0.0218	0.0002	0.0060	0.0003	1.16	0.0004	139	1
T13.9	5	212	0.0488	0.0026	0.1455	0.0078	0.0216	0.0001	0.0059	0.0003	1.22	0.0035	138	1
T13.10	11	411	0.0487	0.0018	0.1478	0.0056	0.0220	0.0001	0.0059	0.0003	1.37	0.0030	140	1
T13.11	15	561	0.0470	0.0011	0.1401	0.0032	0.0216	0.0001	0.0054	0.0003	1.40	0.0014	138	1
T13.12	18	698	0.0487	0.0009	0.1455	0.0026	0.0217	0.0001	0.0055	0.0003	1.27	0.0012	138	1
T13.13	3	105	0.0489	0.0065	0.1483	0.0194	0.0220	0.0002	0.0059	0.0003	1.48	0.0012	140	1
T13.14	5	143	0.0494	0.0035	0.1736	0.0124	0.0255	0.0002	0.0065	0.0003	1.61	0.0058	162	1
T13.15	1	47	0.0480	0.0135	0.1467	0.0344	0.0222	0.0004	0.0059	0.0004	1.20	0.0010	141	3
T13.16	10	447	0.0488	0.0014	0.1470	0.0044	0.0218	0.0001	0.0053	0.0003	0.32	0.0008	139	1
T13.17	4	133	0.0408	0.0058	0.1229	0.0172	0.0219	0.0002	0.0052	0.0003	1.91	0.0013	139	1
T13.18	5	186	0.0491	0.0034	0.1470	0.0103	0.0217	0.0001	0.0051	0.0003	1.90	0.0033	139	1

2011). Precambrian units include moderately high-grade metamorphic rocks such as mica-schist and gneiss dated at 1000–800 Ma (Li *et al.* 1996; Shu and Charvet 1996; Shu *et al.* 2006). Cambrian and Ordovician rock assemblages are mainly sandstone, mudstone and carbonaceous mudstone. The Silurian system is absent. Devonian, Carboniferous and Permian strata consist of shallow marine to littoral facies clastic rocks, limestone and dolomite. Lower Triassic series consist of muddy limestone and shale, whereas Middle Triassic strata are absent in most areas of the Wuyi Mountains (Shu *et al.* 2009; Wang *et al.* 2002; Zhou *et al.* 2002).

The Wuyi Mountains are well-represented by Late Mesozoic volcanic rocks and associated clastic strata. Lower Jurassic strata consist of conglomerate and coarse arkosic sandstone, quartz sandstone and siltstone with carbonaceous mudstone and coal-bed intercalations; Middle Jurassic strata are composed of terrestrial clastic rocks and bimodal volcanic rocks; Upper Jurassic strata consist of andesite and rhyolitic tuffs and tuffaceous siltstone with an age of ~160 Ma (JBGMED 1982; Liu 1985; Ye 1987). Lower Cretaceous strata include rhyolitic welded tuffs with basalt intercalations and a U–Pb geochronological range of 143–139 Ma (Yu *et al.* 2006). Upper Cretaceous siltstone and mudstone are interbedded with intercalated gypsum-bearing layers and basalt, the latter with an age of 105–98 Ma (Yu *et al.* 2001; Wang *et al.* 2002). Paleogene strata are composed

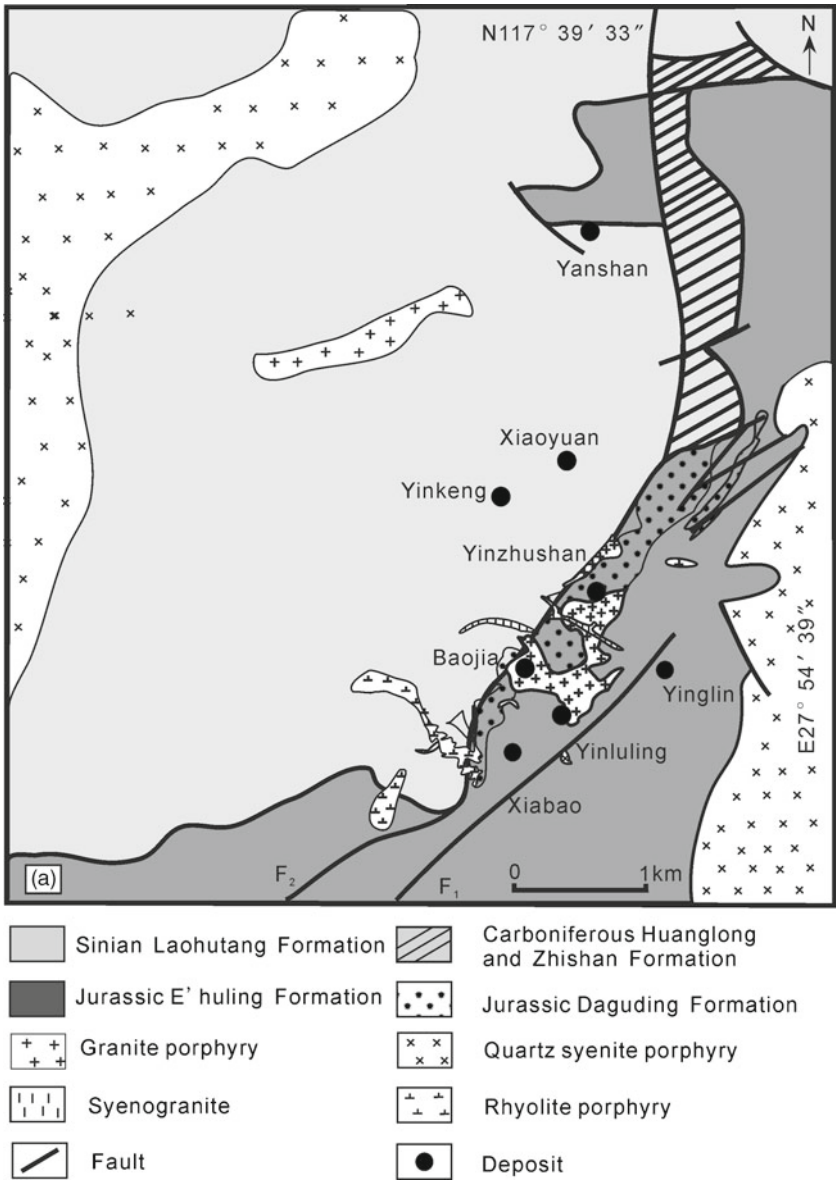

Figure 2. Tectonic framework of the Lengshuikeng ore district (modified after Wang *et al.* 2011).

of coarse clastic rocks, siltstone and mudstone with intercalated gypsum and oil-bearing shale. Neogene strata (siltstones) are rarely developed.

2.3 *Structures*

The SJ fault (figure 1b) in the northern Wuyi uplift belt represents the suture zone between the Cathysian and Yangtze blocks. Geophysical and remote sensing data suggest that the SJ fault cuts deeply into the lower crust and upper mantle (Yang and Luo 1998; Wang *et al.* 2010a, 2011).

The most prominent structural features in the Lengshuikeng ore district are reverse faults. The footwall of the reverse F_2 fault displays a normal stratigraphic sequence of Upper Jurassic strata (dominantly the E'huling, J_3e, Daguding, and J_3d formations), whereas its hanging wall exhibits a sequence of Sinian rocks (the Laohutang Formation, Z_2l). Thrusting may have been initiated during and continuing after the eruption and sedimentation of the Daguding and E'huling formations (Wang *et al.* 2011). The NE-striking reverse F_1 fault has formed before the eruption and sedimentation of the E'huling and Daguding formations. In addition, there are some intraformational fracture zones along the Upper Jurassic stratum, rather than around granitic porphyry. Some of the zones are mineralized and includes Fe–Mn carbonate, quartz-feldspar breccias.

2.4 *Igneous rocks*

SE China is characterized by the Indosinian and the Yanshanian magmatism, which formed a belt of volcanic-intrusive complexes (figure 1b). The Indosinian tectono-magmatism lasted from 240 to 208 Ma (Xie *et al.* 2006; Li *et al.* 2007; Xu *et al.* 2010). The Yanshanian igneous rocks fall into two main age groups (Jahn *et al.* 1976; Chen 1999; Li 2000; Xu *et al.* 2010), namely, Early Yanshanian (208–145 Ma) and Late Yanshanian (145–90 Ma). For example, the Dexing porphyries were emplaced in the early Middle Jurassic (171–170 Ma) as I-type granites (Zhou *et al.* 2012). Besides the Middle Jurassic porphyries at Dexing, there exist a series of Early Cretaceous (129–122 Ma) granitic plutons in this region (figure 1c). These plutons are composed of S-type granites (E'hu pluton) and A-type granites (e.g., Damaoshan and Tongshan plutons) (Jiang *et al.* 2011).

The Middle Jurassic and Early Cretaceous magmatic suites are exposed in the Lengshuikeng ore district. The Jurassic igneous rocks are mainly granitic porphyries with ages ranging from 162 to 155 Ma (U–Pb; Meng *et al.* 2007; Wang *et al.* 2011). The Cretaceous igneous rocks include quartz syenite porphyry, rhyolite porphyry, syenogranite and other mafic dykes (figure 2).

3. Sample descriptions and analytical methods

3.1 *Sampling and petrology*

All samples (∼2 kg each) that were analyzed in this study were collected from outcrops, underground workings (−80 m and −120 m levels) and no. 13911 drill hole (376.4 m depth) in the Lengshuikeng ore district. In the outer peripheral (or distal) zone far away ∼300 m from the ore bodies, the samples of the granite porphyry and rhyolitic tuff show weakly sericite and carbonate alteration. In an inner (or proximal) zone, those near the ore bodies show strongly pervasive hydrothermal alteration, such as chloritization, sericitization, silicification and carbonatization. Samples (T2, T3, No1, PD80-2, PD80-3, PD152-13, and ZK403) with slight alteration and only samples (T1 and T12) with medium alteration were chosen for geochemical and U–Pb dating study. The samples (T7 and T13) from syenogranite are unweathered and unaltered. To constrain the age of the host rocks, three samples were collected for zircon crystal dating by means of the U–Pb method. A sample T1 was collected from the Yinzhushan granite porphyry in the Lengshuikeng ore district. The Lengshuikeng granite porphyry contains phenocrysts (15–35%) of quartz, plagioclase, K-feldspar and biotite in a groundmass (65–85%) of subhedral K-feldspar, quartz, plagioclase and minor biotite. The principal minerals include quartz (∼51%), K-feldspar (∼35%), plagioclase (∼10%), biotite (∼1%) and alkaline-augite (∼2%). Accessory minerals (∼1%) are mainly magnetite, zircon and apatite. A sample T3 was collected from the Daguding Formation in the Lengshuikeng ore district. It is a medium-fine grained (0.5–2.0 mm) rhyolitic tuff, which is light gray and off-white, and composed of angular grains (50–60%) of quartz, K-feldspar, plagioclase, biotite, with minor glass shards and cuttings, all set in a fine matrix (ca. 40–50%) of volcanic ash and glass shards. A sample T13 was collected from the Lengshuikeng syenogranite, which cuts through both the granite porphyry and the Mesozoic strata. It is pink and has a massive structure and a porphyritic texture. It is composed of K-feldspar and/or microcline (30–45%), perthite (5–10%), quartz (∼30%), plagioclase (∼10%), other dark minerals (∼4%) including amphibole and biotite, and minor muscovite and pyroxene. Accessory minerals (∼1%) include zircon, apatite, titanite, and Fe–Ti oxide. Some hornblende grains are enclosed within K-feldspar.

3.2 *Analytical methods*

Zircon grains were separated from each rock sample at the Beijing Research Institute of Uranium Geology. Crushing was performed using a standard jaw crusher followed by a disc grinder. Density separation of heavy minerals was achieved using a Wilfley table. Heavy minerals were then passed through a hand-magnet and Frantz magnetic separator before separation using heavy liquids. The most non-magnetic zircon grains were then hand-picked under a binocular microscope according to their clarity (free of inclusions) and morphology. A large split of samples of zircon grains (generally 1000–2000 grains) was incorporated into a 1-inch epoxy mount together with fragments of a 91,500 standard zircon (age 1064 Ma) and NIST612 silicate glass. The mounts were sanded down to a thickness of ~20 μm, polished, imaged, and cleaned prior to isotopic analysis. Reflected and transmitted light photomicrographs were prepared for all zircons at the State Key Laboratory of Continental Dynamics, Northwest University. Cathodoluminescence (CL) images were acquired at the Institute of Mineral Resources, Chinese Academy of Geological Sciences, using a JOEL JXA 8800R, at 20 kV, 10 nA. The CL images were used to decipher the internal structures of the sectioned grains and to ensure that the 10 μm of LA-MC-ICP-MS spot was wholly within a single age component within the sectioned grains.

U–Pb dating of zircons was conducted by LA-MC-ICP-MS at the Tianjin Institute of Geology and Mineral Resources, Tianjin, China. The analyses involve ablation of zircon with a NUP193-FX ArF Excimer laser (operating at a wavelength of 193 nm) using a spot diameter of 35 μm, with constant 13–14 J/cm^2 energy density, and a repetition rate of 8–10 Hz. The ablation pits measure ~12 μm in depth. The ablated material is carried in He into the plasma source of a GVI Isoprobe, which is equipped with a flight tube of sufficient width such that U, Th, and Pb isotopes can be measured simultaneously. All measurements were made in static mode, using Faraday detectors with 10e11 Ω resistors for ^{238}U, ^{232}Th, ^{208}Pb, and ^{206}Pb, a Faraday detector with a 10e12 Ω resistor for ^{207}Pb, and an ion-counting channel for ^{204}Pb (e.g., Gehrels *et al.* 2006; Raharimahefa and Kusky 2010). Ion yields are ~1.0 mV/ppm. Each analysis consisted of one 12-s integration on peaks

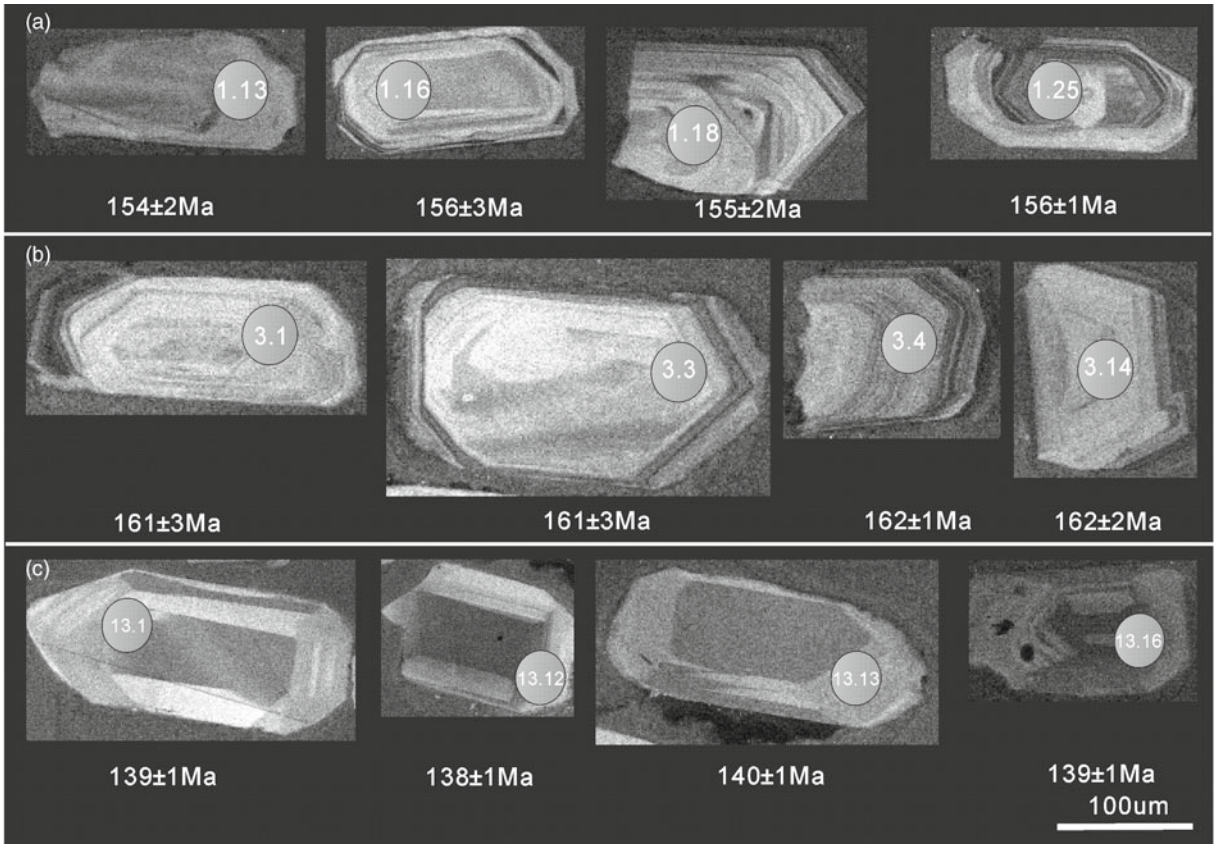

Figure 3. Representative cathodoluminescence images of zircons from granite porphyry, rhyolitic tuff, and syenogranite in the Lengshuikeng ore district.

with the laser off (for backgrounds), 12 1-s integrations with the laser firing, and a 30 s delay to purge the previous sample and prepare for the next analysis. Errors in determining $^{206}Pb/^{238}U$ and $^{206}Pb/^{204}Pb$ resulted in an error of 1–4% (at 1-sigma level) in $^{206}Pb/^{238}U$ age per analysis. A common Pb correction is achieved by using the measured ^{204}Pb and assuming an initial Pb composition from Stacey and Kramers (1975) (with uncertainties of 1.0 for $^{206}Pb/^{204}Pb$ and 0.3 for $^{207}Pb/^{204}Pb$). However, because backgrounds were measured on peaks (thereby subtracting any background ^{204}Hg and ^{204}Pb) and because very little Hg is present in the argon gas (background ^{204}Hg = ~300 CPS), our measurements of ^{204}Pb were unaffected by the presence of ^{204}Hg.

Geochemical analyses of rock samples were carried out at the Beijing Research Institute of Uranium Geology, China. Major elements were determined by standard X-ray fluorescence (XRF). Samples were prepared as glass discs using a Rigaku desktop fusion machine. Analyses were performed on a Rigaku ZSX100e instrument at GIG–CAS. Trace elements were determined by induced coupled plasma mass spectrometry (ICP–MS) on Finnigan MAT (Element I) instrument. About 100 mg of each sample were weighted in Teflon beakers and then leached by 1.0 ml HF under an ultrasonic bath for several hours to dissolve silicates in the samples. The residues were dissolved in 1.0 ml HF and 0.6 ml HNO_3 on a hotplate at ca. 190°C overnight to digest sulphide and phosphate fractions. After dissolution, the sample solutions were centrifuged and the supernatants were transferred to clean Teflon beakers. Then, the solutions were evaporated to near dryness, 1.0 ml concentrated HNO_3 was added and dried twice to get rid of the HF or HCl in the samples. Finally, all samples were dissolved in 5% HNO_3 solution spiked with an internal standard Rh (10 ppb) for analysis. Analytical uncertainties for either major or trace elements are mostly between 1% and 5%.

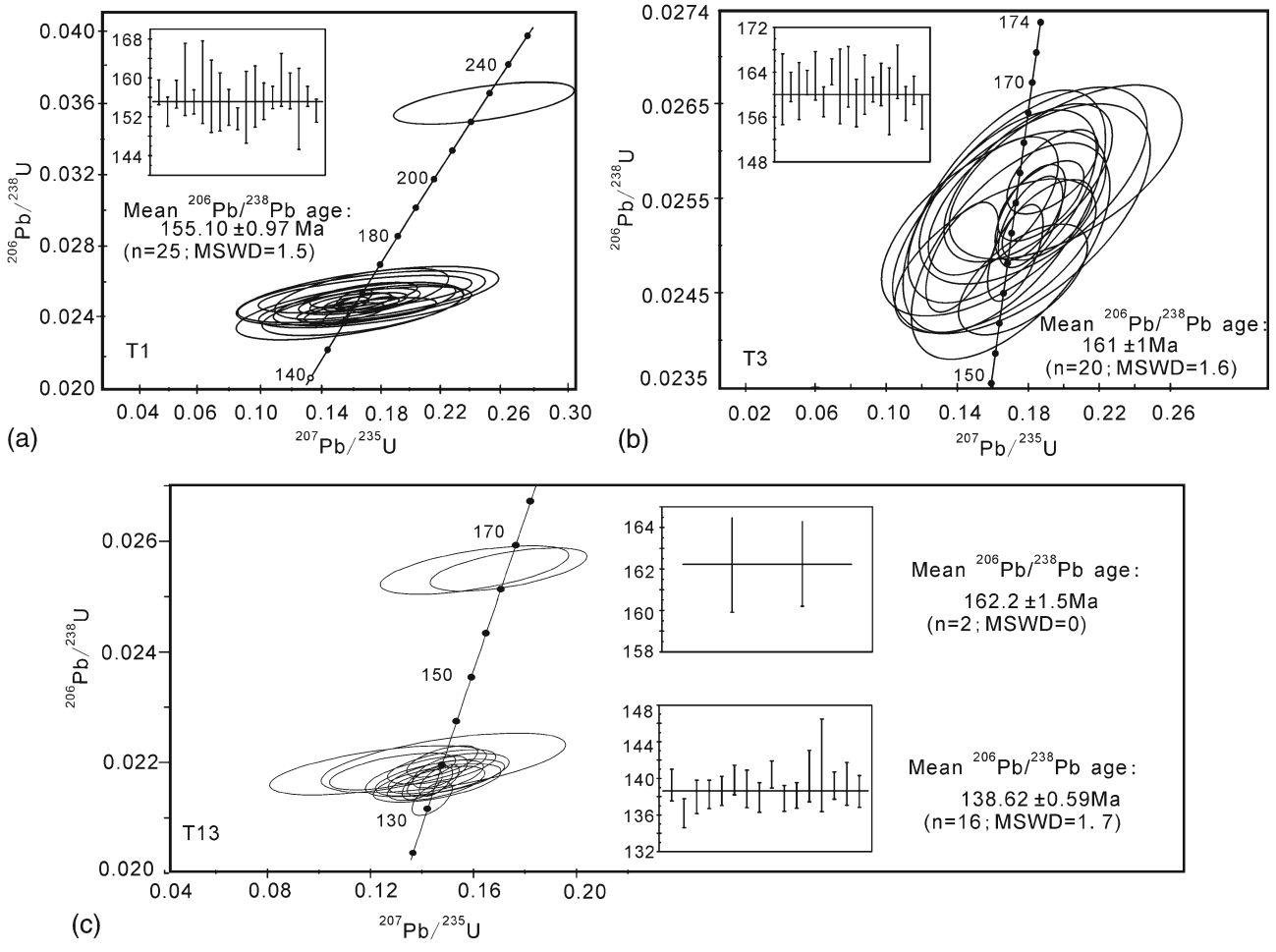

Figure 4. Zircon U–Pb concordia plots and calculated weighted mean $^{206}Pb/^{238}U$ ages for rocks from the Lengshuikeng ore district: (**a**) Sample T1 granite porphyry; (**b**) Sample T3 rhyolitic tuff; and (**c**) Sample T13 syenogranite. Data-point error ellipses are 2σ (sigma) for U–Pb concordia diagrams, and data-point error symbols are 2σ (sigma) for weighted mean diagrams. Data are from table 1.

Table 2. *Major elements (wt%) and trace elements (μg/g) analytical results for rocks from the Lengshuikeng ore district. Note:* $\delta = (Na_2O + K_2O)^2/(SiO_2 - 43)$; $AR = (Al_2O_3 + CaO + Na_2O + K_2O)/(Al_2O_3 + CaO - Na_2O - K_2O)$.

	Tuff				Granite porphyry					Syenogranite	
	T3	No1	PD80-2	T12	PD80-3	T1	T2	PD152-13	ZK403	T7	T13
SiO_2	74.73	73.81	76.43	78.02	75.62	77.05	73.20	71.41	69.96	75.90	77.25
TiO_2	0.27	0.08	0.08	0.03	0.10	0.15	0.26	0.33	0.34	0.10	0.15
Al_2O_3	13.23	13.46	10.55	14.20	12.79	9.01	12.44	14.28	14.86	12.41	12.57
Fe_2O_3	1.59	4.01	2.81	0.89	2.65	5.14	2.57	1.28	1.85	1.57	0.54
FeO	0.10	3.50	0.90	0.15	0.90	0.45	1.50	1.15	1.60	0.35	0.10
MnO	0.11	0.12	0.15	0.03	0.21	0.02	1.00	0.27	1.54	0.083	0.01
MgO	0.30	0.18	0.41	0.07	0.53	0.27	0.33	0.14	0.35	0.062	0.10
CaO	0.60	0.10	0.064	0.05	0.11	0.05	0.27	0.22	0.30	0.073	0.05
Na_2O	1.70	0.23	0.30	0.09	0.11	0.08	0.72	0.40	0.19	2.49	1.98
K_2O	5.14	4.47	2.91	3.83	3.58	2.22	5.88	8.99	6.97	5.83	5.61
P_2O_5	0.07	0.02	0.01	0.01	0.04	0.01	0.07	0.10	0.11	0.01	0.02
LOI	2.08	0.93	4.44	2.73	4.22	6.01	3.10	2.26	3.32	1.28	1.53
Total	99.92	100.92	99.06	97.31	100.86	96.84	98.19	98.58	98.09	98.80	98.34
δ	1.47	0.72	0.31	0.44	0.42	0.16	1.44	3.10	1.90	2.10	1.68
A.R.	2.96	2.06	1.87	1.76	1.80	1.68	3.16	4.68	2.79	2.33	4.02
A/CNK	1.40	2.49	2.81	3.16	3.00	3.44	1.54	1.33	1.78	1.18	1.32
Rb	233.00	186.00	163.00	323.00	185.00	120.00	241.00	298.00	268.00	285.00	227.00
Ba	675.00	544.00	122.00	13.40	202.00	88.90	632.00	1240.00	971.00	119.00	391.00
Ga	18.50	19.30	21.40	19.50	13.10	19.50	18.80	24.30	16.40	19.10	18.50
Th	28.80	24.50	19.40	27.10	24.00	10.20	29.50	25.00	22.20	47.20	38.50
U	3.93	7.46	6.08	5.32	6.74	7.39	3.52	3.45	3.94	6.67	4.45
Nb	23.30	23.20	19.10	49.00	20.30	22.10	22.50	20.70	21.00	37.20	25.40
Ta	1.63	2.33	1.84	3.63	1.99	2.06	1.56	1.31	1.31	2.57	2.73
Sr	44.70	18.40	6.71	1.79	10.20	2.63	31.10	57.80	49.40	24.10	13.10
Zr	162.00	147.00	147.00	209.00	132.00	144.00	151.00	166.00	155.00	417.00	566.00
Hf	5.59	5.42	4.90	10.30	4.96	5.64	5.12	5.25	4.47	13.70	15.70
Y	24.3	22.40	18.50	48.70	16.40	24.30	25.10	22.30	21.00	57.30	29.20
La	47.00	26.70	25.50	1.95	31.70	20.60	52.60	63.60	61.40	89.20	87.80
Ce	86.90	52.50	48.10	3.95	62.20	43.10	98.50	118.00	115.00	165.00	96.60
Pr	9.78	6.06	5.47	0.66	7.36	5.16	10.80	12.80	12.30	19.10	16.40
Nd	36.10	23.50	20.00	3.16	25.10	20.50	39.00	44.70	41.60	67.10	54.70
Sm	6.66	4.76	4.30	1.59	5.02	4.64	7.00	7.32	6.40	12.90	7.05
Eu	1.00	0.84	0.69	0.02	0.73	0.87	1.04	1.28	1.31	0.14	0.29
Gd	5.34	4.16	3.60	2.95	3.85	4.14	5.72	5.37	5.19	11.10	5.19
Tb	0.85	0.74	0.63	0.993	0.62	0.83	0.89	0.83	0.77	1.83	0.81
Dy	4.86	4.06	3.59	7.82	3.24	4.78	4.87	4.57	4.31	11.50	5.56
Ho	0.88	0.73	0.66	1.62	0.60	0.84	0.85	0.78	0.75	2.05	1.09
Er	2.41	2.10	2.02	5.73	1.74	2.19	2.44	2.20	2.05	6.24	3.48
Tm	0.38	0.35	0.32	1.00	0.28	0.35	0.37	0.35	0.33	1.01	0.60
Yb	2.39	2.27	2.01	6.23	1.78	2.09	2.38	2.14	1.88	6.45	3.88
Lu	0.36	0.34	0.31	0.92	0.26	0.33	0.35	0.32	0.28	0.98	0.61
ΣREE	204.92	129.10	117.19	38.59	144.47	110.42	226.81	264.27	253.57	394.60	284.05
LREE/HREE	10.73	7.75	7.93	0.42	10.68	6.10	11.69	14.95	15.30	8.59	12.39
Ce/Yb_N	9.40	5.98	6.19	0.16	10.70	5.33	9.04	14.26	15.81	6.62	6.44
(Nb/Ta)N	9.96	14.29	10.38	13.50	10.20	10.73	14.42	15.80	16.03	14.48	9.30
Zr + Nb + Ce + Y	296.50	245.10	232.70	230.90	233.50	297.10	327.00	312.00	321.00	676.50	717.20
10000∗Ga/Al	2.64	2.71	3.83	2.88	2.75	2.96	2.49	3.09	2.34	2.91	2.78
Eu/Eu*	0.50	0.56	0.52	0.02	0.49	0.59	0.49	0.60	0.67	0.03	0.14

4. Results

4.1 *Zircon U–Pb geochronology*

Zircons in the Lengshuikeng granite porphyry, rhyolitic tuff, and syenogranite are colourless or buff to transparent, euhedral to subhedral, elongate to stubby grains. In the CL images, they show obvious oscillatory zoning typical of magmatic grains (figure 3). Measured $^{206}Pb/^{238}U$ ages from individual zircons are shown in figure 3 and the analytical results of U–Pb dating are listed in table 1. Uncertainties shown in these tables are at the 1-sigma level, and include only measurement errors. Data of Th/U ratios from the granite porphyry, rhyolitic tuff, and syenogranite vary between 0.32 and 2.41 (table 1), suggesting their magmatic origins (Hoskin and Black 2000; Belousova *et al.* 2002; Zhou *et al.* 2002). Thus, the U–Pb ages of the zircons are likely the crystallization ages of the rocks.

The U–Pb concordia diagrams for the granite porphyry, rhyolitic tuff, and syenogranite zircon analyses are shown in figure 4. Twenty-five out of 26 analyses of zircons from the granite porphyry sample T1 form a tight cluster, with a weighted mean $^{206}Pb/^{238}U$ age of 155.1 ± 0.97 Ma (2σ, MSWD = 1.5; figure 4a). For the rhyolitic tuff (sample T3), all the analyses from 20 spots cluster close to concordia, with a weighted mean $^{206}Pb/^{238}U$ age of 161.0 ± 1.0 Ma (2σ, MSWD = 1.6; figure 4b). Sixteen analyses of zircons from syenogranite sample T13 plot in-group on the concordant curve and give a weighted mean $^{206}Pb/^{238}U$ age of 138.62 ± 0.59 (2σ, MSWD = 1.7; figure 4c). Two other analyses of zircons from syenogranite sample T13 also plot on the concordant curve but show higher $^{206}Pb/^{238}U$ ages, with a weighted mean $^{206}Pb/^{238}U$ age of 162.2 ± 1.5 Ma (2σ) (MSWD = 0; figure 4c).

4.2 *Bulk-rock geochemistry*

4.2.1 *Alteration effects*

Petrographic examination indicates that the samples of granite porphyry and rhyolitic tuff show different degrees of alteration. This observation is supported by the differences in total major element contents and LOI values of the samples of granite porphyry and rhyolitic tuff (table 2). The 'missing wt%' likely represents analytical error and/or unmeasured substances enriched or depleted due to alteration effect. However, some major elements such as Ti, Fe, and P, high-field-strength elements (HFSE), rare earth elements (REE), and transition elements have long been used as petrogenic tracers to classify igneous rocks and their tectonic settings and to distinguish the protoliths of metamorphic or altered rocks based on the general immobile nature of these elements in most geologic settings (e.g., Zhou 1999). In contrast, Ca, Na, K, and large ion lithophile elements (LILE) (e.g., Rb, Sr, and Ba) are generally mobile (e.g., Smith and Smith 1976; Hickmott *et al.* 1992; Zhou 1999). In addition, Mg is thought to be easily transported in solution and its content will be changed by alteration in some mafic rocks containing olivine

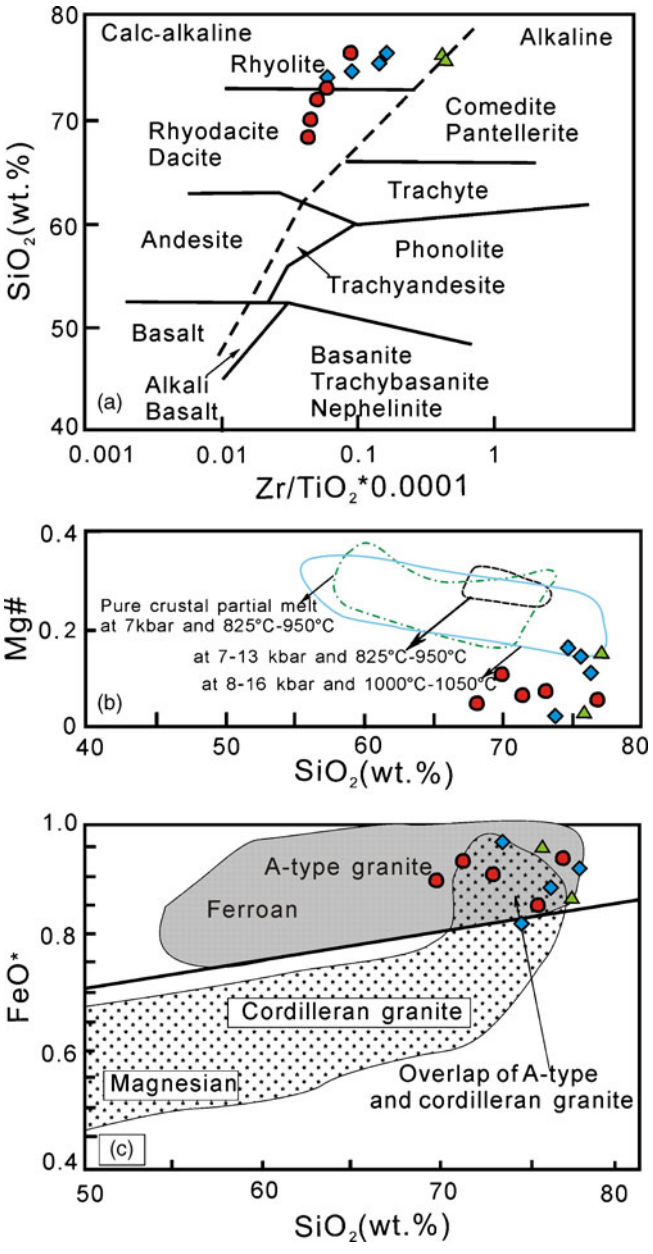

Figure 5. (**a**) Zr/TiO_2 *vs.* SiO_2 diagram; (**b**) Mg# [=Mg/(Mg + Fe*)] *vs.* SiO_2 diagram; and (**c**) FeO* (FeO*/(FeO*+MgO)) *vs.* SiO_2 diagram. In (a), the dashed line separates calc-alkaline and alkaline compositions (Winchester and Floyd 1977). In (b), the field of pure crustal partial melt is from Rapp and Watson (1995). In (c), the composition range for rocks from Frost *et al.* (2001). Data are from table 2.

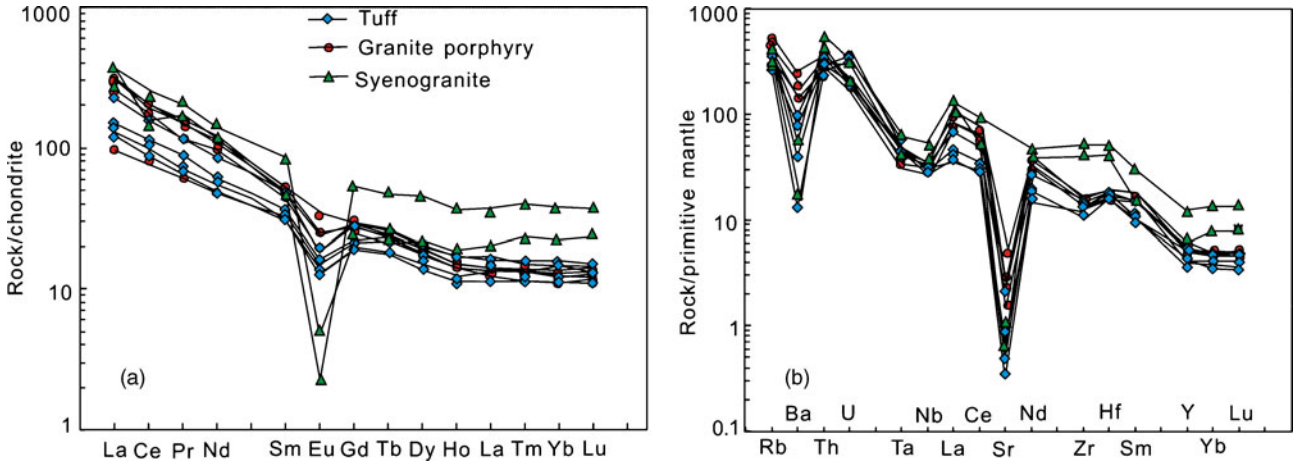

Figure 6. (**a**) Chondrite-normalized REE patterns and (**b**) primitive mantle-normalized trace element spider diagram for the granite porphyry and rhyolitic tuff from the Lengshuikeng ore district. Chondrite and primitive mantle values are from Sun and McDonough (1989). Data are from table 2.

and pyroxene, but it tends to be immobile and will not be greatly affected by alteration in intermediate acid igneous rocks due to the lack of olivine and pyroxene (e.g., Zhou 1999). Therefore, in the following discussion below, we used all elements for the unaltered syenogranite samples but we used only immobile elements such as Fe_2O_3, MgO, HFSE (Ti, Zr, Y, Nb, Ta, Hf), REE for the variously altered granite porphyry and altered rhyolitic tuff samples.

4.2.2 *Major and trace element compositions*

The granite porphyries consist mainly of granodiorite-porphyry of the calc-alkaline series with iron-enriched characteristics (figure 5). The granite porphyry samples show unusually low Na_2O values (table 2) compared to normal granites, indicating the effect of alteration. The granite porphyries have high REE concentrations (ΣREE = 110–264 ppm; average of ∼191 ppm) with chondrite-normalized La/Yb ratios of 7–24 and chondrite-normalized La/Sm ratios of 4–10. They exhibit LREE enrichment (LREE/HREE = 6–15; average of ∼12) with negative Eu anomalies (Eu/Eu* = 0.49–0.67) (figure 6a), probably indicating the fractional crystallization of plagioclase. They are depleted in HFSE, showing notable negative Ta–Nb anomalies (figure 6b). The Lengshuikeng granite porphyries show markedly decreasing values of P_2O_5, La, Ce and Th with increasing SiO_2 content (figure 7a–d).

Among the rhyolitic tuff samples, sample T12 has lowest ΣREE and Eu/Eu* (table 2) owing to strong effect of alteration. Therefore, sample T12 is excluded in the following discussion of the geochemistry of Lengshuikeng rhyolitic tuffs. Their composition is that of rhyolite of the calc-alkaline series with iron-enriched characteristics (figure 5). The rhyolitic tuffs have high REE concentrations (ΣREE = 117–205 ppm; average of ∼150 ppm). They exhibit LREE enrichment (LREE/HREE = 7–11; average of ∼9) with negative Eu anomalies (Eu/Eu* = 0.50–0.56) (figure 6a), probably indicating the fractional crystallization of plagioclase. They are depleted in HFSE, showing notable negative Ta–Nb anomalies (figure 6b). The Lengshuikeng rhyolitic tuffs show markedly decreasing values of P_2O_5, La, Ce, and Th with increasing SiO_2 content (figure 7a–d). The major and trace element compositions of the rhyolitic tuffs are remarkably similar to those of the granite porphyries.

The Lengshuikeng syenogranites are strongly peraluminous (A/CNK>1.10) (table 2). They are alkali-rich (figure 5), with very low P_2O_5 content and very high Th, La, Ce and Zr contents (figure 7) compared to the granite porphyries and rhyolitic tuffs. The Lengshuikeng syenogranites, compared to the granite porphyries and rhyolitic tuffs, have higher Ga/Al ratios (>2.7) and ΣREE contents (table 2) but are more depleted in Eu and, thus, show stronger negative Eu anomalies (table 2; figure 6a). They are also depleted in Ba and Sr, with significant negative Ba and Sr anomalies (figure 6b). The syenogranites have HFSE contents higher than those of the granite porphyries.

5. Discussion

5.1 *Timing of magmatism and host rock*

The LA-MC-ICP-MS zircon U–Pb age (161.0 ± 1.0 Ma) obtained from the Lengshuikeng rhyolitic

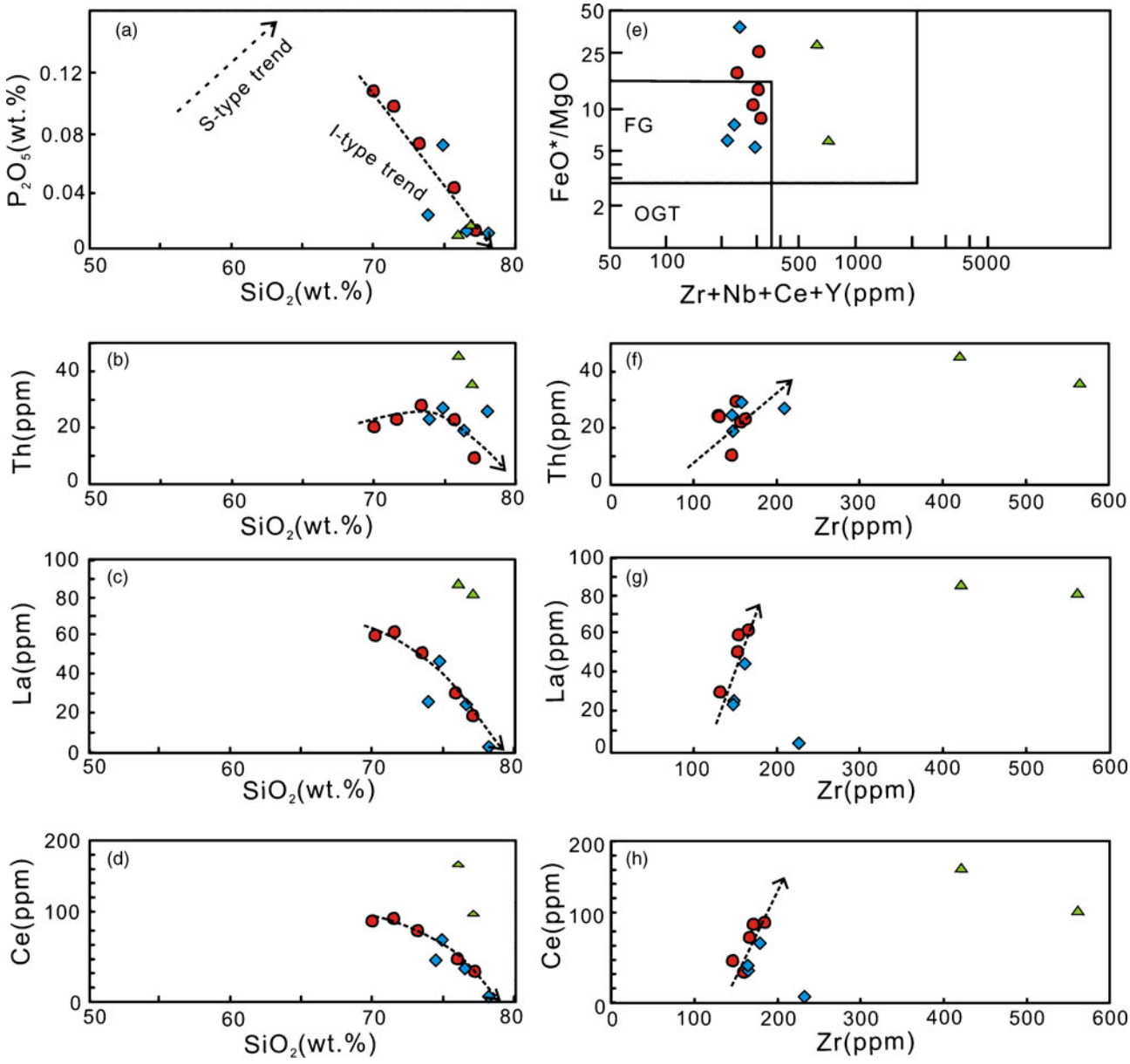

Figure 7. (**a**) SiO_2 *vs.* P_2O_5 diagram; (**b**) SiO_2 *vs.* Th diagram; (**c**) SiO_2 *vs.* La diagram; (**d**) SiO_2 *vs.* Ce diagram; (**e**) FeO*/MgO *vs.* Zr + Nb + Ce + Y diagram (Whalen *et al.* 1987); (**f**) Zr *vs.* Th diagram; (**g**) Zr *vs.* La diagram; and (**h**) Zr *vs.* Ce diagram. The Lengshuikeng syenogranites are typical of A-type granites, whereas most of the other samples fall into the fractionated field. FG = fractionated M-, I- and S-type felsic granites; OGT = unfractionated M-, I- and S-type granites. Symbols are as in figure 6. Data are from table 2.

tuff samples confirm the age of the Daguding Formation. Previously reported the ages of the Daguding Formation in Jiangxi Province include a K–Ar age of 141 Ma for rhyolite ignimbrite in the Dongxiang County (JBGMED 1982) and a K–Ar age of 165 Ma for rhyolitic tuff in the Xiangshan deposit (Ye 1987). Previously reported ages of the E'huling Formation in Jiangxi Province include a whole-rock Rb–Sr age of 142 ± 1 Ma for andesite, andesitic tuff, rhyolite ignimbrite, rhyolite, and crystal tuff in the Shangqinggong area (NGST 1997) and a whole-rock K–Ar age of 135 Ma for tuff in the Yiyang County (NGST 1997). The 161 Ma age of the Lengshuikeng rhyolitic tuff obtained in this study can be interpreted as the timing of magmatic crystallization of the zircons and broadly corresponding to the deposition of the rhyolite tuff, which is about 5 Ma earlier than that of the Lengshuikeng granite porphyry.

The LA-MC-ICP-MS U–Pb data on zircons from the Lengshuikeng granite porphyry indicate crystallization at 155.10 ± 0.97 Ma. In contrast, Meng *et al.* (2007) have reported a whole-rock Rb–Sr age of 159 Ma whereas Zuo *et al.* (2010) have

reported a SHRIMP U–Pb age of 162.0 ± 2 Ma for the Lengshuikeng granitic porphyry. However, the Lengshuikeng granite porphyry intruded into the Daguding and E'huling formations. It follows that the age of the Lengshuikeng granite porphyry should be younger than that of the Daguding Formation. Therefore, the SHRIMP U–Pb age of 162.0 ± 2 Ma does not support field relationships of the rocks and is most probably caused by inherited older zircons. In addition, the zircon U–Pb age (155.10 ± 0.97 Ma) obtained in this study corresponds to the peak period (∼155 Ma) of magmatic activities in SE China (Mckee *et al.* 1987; Pan and Dong 1999; Yin *et al.* 2002; Mao *et al.* 2003; Meng *et al.* 2009; Xu *et al.* 2010).

The ages of 138.62 ± 0.59 Ma and 162.2 ± 1.5 Ma of LA-MC-ICP-MS zircon U–Pb dating have been obtained for the syenogranite. The zircon U–Pb age of 138.62 ± 0.59 Ma obtained from the syenogranite likely represents crystallization age of magma, whereas the zircon U–Pb age of 162.2 ± 1.5 Ma obtained from the same rock may be interpreted as an inherited age. That is because the latter age data correspond with Th/U ratios that are distinct from those that correspond with the former age data.

Sericite K–Ar ages of 121–138 Ma and K-feldspar K–Ar age of 136.5 Ma have been obtained from the Lengshuikeng granite porphyry (NGST 1997). Our new age data from the granite porphyry and rhyolitic tuff demonstrate that those previously reported K–Ar ages have underestimated the timing of magmatism but likely represent subsequent hydrothermal alteration of rock-forming minerals. This subsequent hydrothermal alteration may be associated with the syenogranite, based on our new age data.

5.2 *Host rock of mineralization*

From some deposits associated with granitic porphyries in the Jiangxi Province, previously reported Re–Os model ages include 150.2 ± 2.2 Ma for the quartz–vein Mo–W Hukeng deposit (Liu *et al.* 2008), 152 ± 20 Ma for the Xiongjiashan Mo deposit (Meng *et al.* 2007), 154.4 ± 3.4 Ma for the Taoxikeng Mo deposit (Chen *et al.* 2006) and 156.3 ± 4.8 Ma for the Xingluokeng Mo deposit (Zhang *et al.* 2008). In addition, Zhang *et al.* (2009) have reported Rb–Sr dating of sphalerite with an isochron age of 135.5 ± 5.7 Ma in the Jinzhuping Mo deposit. Therefore, on the basis of the relationship between the above-mentioned deposits and granitic porphyries, the Lengshuikeng mineralization is considered to be part of a Mesozoic large-scale magmatic-mineralization event.

5.3 *Genetic types and sources of magma*

5.3.1 *Genetic type*

Granitic rocks have commonly been divided into three types according to the nature of their protolith and their petrographical and geochemical features, e.g., I- and S-type granites (Chappell and White 1974) and A-type granites (Loiselle and Wones 1979). However, the distinction between different types of granites is not always straightforward, especially for the highly fractionated granites. Generally, S-type granites are strongly peraluminous, contain abundant Al-rich minerals such as primary muscovite, garnet and cordierite (e.g., Chappell and White 1974; Miller 1995; Frost *et al.* 2001, 2002; Clemens 2003). These characteristics are not found in the Lengshuikeng granite porphyries and rhyolitic tuffs. In addition, the Fe* *vs.* SiO_2 diagram does not yield unambiguous information for the genetic type of the Lengshuikeng granite porphyries because the samples plot mostly within or close to the overlap between fields for A-type and Cordilleran granites (figure 5c). In contrast, the P_2O_5 *vs.* SiO_2 contents of the Lengshuikeng granite porphyries (figure 7a) indicate their affinity with I-type granites (figure 7a) and most of the samples of granite porphyry and rhyolitic tuff from Lengshuikeng fall in the field of fractionated granites in the (FeO*/MgO) *vs.* (Zr + Nb + Ce + Y) diagram (figure 7e).

The geological and geochemical characteristics of the Lengshuikeng syenogranites strongly suggest their affinity with A-type granites. Petrographically, these syenogranites contain interstitial mafic minerals. Geochemically, they are enriched in alkalis (figure 5a), REE (except for Eu, figure 6a) and HFSE, but depleted in Ba and Sr (figure 6b). These features, which are typical of A-type granites, have been recognized by many researchers (e.g., Collins *et al.* 1982; Whalen *et al.* 1987; Eby 1992). The two samples of syenogranites from Lengshuikeng fall in the field of A-type granites in the Fe* *vs.* SiO_2 diagram (figure 5c) and in the field of fractionated granites in the (FeO*/MgO) *vs.* (Zr + Nb + Ce + Y) diagram (figure 7e).

5.3.2 *Magma sources*

Data of Nd isotopic compositions of the Lengshuikeng granite porphyries, which are from Meng *et al.* (2007), show a narrow range of εNd values (−10.2 to −8.5). The Lengshuikeng granite porphyries have negative εNd(t) values with corresponding crust residual ages of 1.74–1.77 Ga (Meng *et al.* 2007), suggesting that they might have been derived from re-melting of Proterozoic infracrustal metasedimentary rocks. In addition,

the available Nd isotopic data show that the highest εNd(t) value for the Lengshuikeng granites is −8.5 (Meng *et al.* 2007), which is lower than that of the basic metaigneous rocks in the Cathaysia block–Mayuan Group amphibolite with εNd(t) values of −1.7 to 1.2 (Yuan and Wu 1991). This indicates that the Lengshuikeng granite porphyries are unlikely derived from partial melting of infracrustal basic metaigneous rocks mixed with mantle-derived magmas. Moreover, basaltic rocks in the Cathaysia block are sparsely distributed, so it is also unlikely that such extensive granite porphyries were produced by differentiation of basaltic magma. Recently, many researchers proposed that I-type granites are derived from remelting of sedimentary rocks reformed by mantle-derived magma (Chappell and Stephens 1988; Sylvester 1998; Clemens 2003), or that the melt compositional change from S- to I-type is caused by gradually decreasing sediment during re-melting of the crust (Collins and Richards 2008). As shown in figure 8, Sr–Nd isotopic compositions for the Lengshuikeng granite porphyries are close to the binary mixed curve between depleted mantle and upper crust end-member, and closer to the upper crust end-member of Cathaysia block. Therefore, the Lengshuikeng granite porphyries were probably derived from partial melting of underlying Proterozoic metasedimentary rocks with mantle-derived magmas.

The Lengshuikeng granite porphyries have essentially consistent εNd(t) values (Meng *et al.* 2007), showing that they have the same provenance. As shown in figure 6(b), the pronounced depletions in Ba, Sr, P, Ti, Nb and Eu demonstrate that advanced fractional crystallization have taken place during the formation of these granites. Commonly, the separation of Ti-bearing phases (such as ilmenite, hornblende and titanite) and apatite results in depletion of Nb, Ti and P (Wu *et al.* 2003). Strong Eu depletion requires extensive fractionation of plagioclase and/or K-feldspar. Previous studies (Wu *et al.* 2003; Xiong *et al.* 2005) indicate that fractionation of plagioclase usually lead to negative Sr and Eu anomalies, and K-feldspar fractionation produce negative Ba and Eu anomalies. The Lengshuikeng granite porphyries show marked decreases in La, Ce and Th with decreasing Zr (figures 7f–h) but with increasing SiO_2 content (figures 7b–d). This feature is usually considered to be an important criterion for fractionation of zircon, allanite and monazite (Bea *et al.* 1994; Ewart and Griffin 1994). The Lengshuikeng granite porphyries have low Nb/Ta ratios of 10.73–16.03 and Zr/Hf ratios of 25.53–34.67 (table 2). Because Nb, Ta, Zr and Hf are generally immobile and not greatly affected by alteration (Dostal and Chatterjee 2000; Jahn *et al.* 2001), the low Nb/Ta (10–17) and Zr/Hf (25–35) ratios of the Lengshuikeng granite porphyries (table 2) suggest that they likely resulted from fractional crystallization. Previous studies indicate that fractionation of manganocolumbite, manganotantalite, and their accessory minerals usually lead to low Nb/Ta ratios (Linnen and Keppler 1997). Therefore, the Lengshuikeng granite porphyries were probably derived from partial melting of underlying Proterozoic metasedimentary

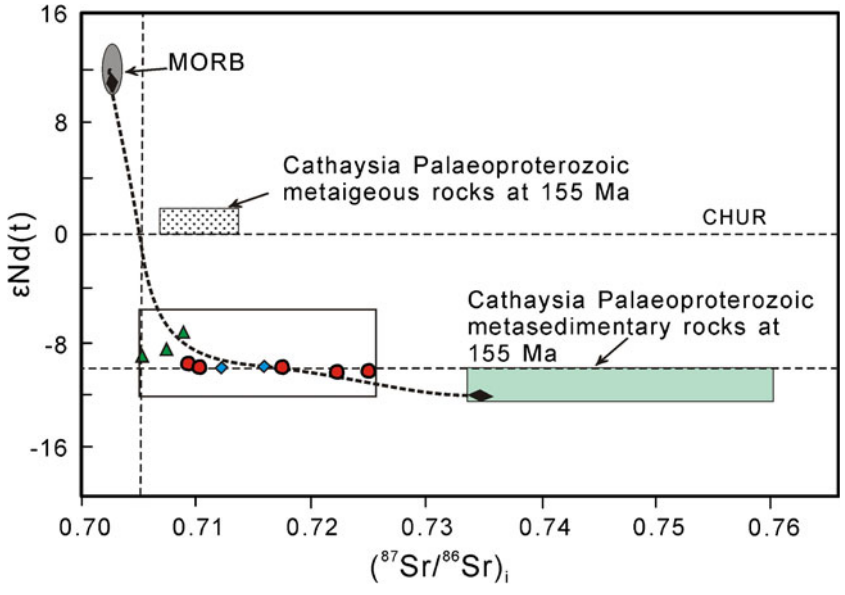

Figure 8. Initial $^{87}Sr/^{86}Sr$ *vs.* εNd(t) diagram. Data for the Lengshuikeng granitic rocks are from Meng *et al.* (2007); MORB is from Faure (1986); Paleoproterozoic metasedimentary and metaigneous rocks are from Yuan and Wu (1991); CHUR is chondritic uniform reservoir.

rocks with mantle-derived magmas, accompanied by fractional crystallization.

Data of Nd isotopic compositions of the Lengshuikeng rhyolitic tuffs, which are from Meng *et al.* (2007), also show a narrow range of εNd values (−9.5 to −9.1). Therefore, the Lengshuikeng granite porphyries and rhyolitic tuffs were likely derived by similar processes and from similar magma sources.

Data Nd isotopic compositions of the Lengshuikeng syenogranites, which are from Meng *et al.* (2007), show a narrow range of εNd values (−7.7 to −7.5). The Lengshuikeng syenogranites have Mesoproterozoic TDM ages of Nd isotopes (1.65–1.70 Ga; Meng *et al.* 2007), suggesting that Proterozoic basement was involved in partial melting at depth. The Lengshuikeng syenogranites are mainly peraluminous, suggesting that metasedimentary rocks were involved in partial melting. They have much higher initial $^{87}Sr/^{86}Sr$ ratios and higher εNd(t) values than Proterozoic metasedimentary rocks at the age of intrusion (figure 8), which requires that the Proterozoic basement was also reformed by mantle-derived magma.

The Lengshuikeng syenogranites have high HREE (Yb > 1.8 ppm, up to 6.45 ppm) and Y (>18 ppm, up to 57.3 ppm) contents and possess flat HREE patterns (figure 6a), which preclude garnet as a residual phase. Marked negative Eu anomalies in these syenogranites (figure 6a) require, therefore, melting of a source rock within the stability field of plagioclase (Jiang *et al.* 2011). This implies that the source regions of the Lengshuikeng syenogranites are relatively shallow (<30 km). These syenogranites show lower Mg# than pure crustal melts (figure 5b), suggesting that the magmas might have undergone subsequent fractionation of mafic minerals, such as biotite, after partial melting.

Therefore, we propose that the granite porphyries, syenogranites and rhyolitic tuffs in the Lengshuikeng ore district were probably derived from the same magma sources, which derived from partial melting of crustal-mantle mixing materials, accompanied by fractional crystallization. The proposition is supported by petrogenetic models for A-type magmas, which involve partial melting of specific crustal protoliths (e.g., Collins *et al.* 1982; Whalen *et al.* 1987; Creaser *et al.* 1991), extensive fractional crystallization from mantle-derived basaltic magmas (e.g., Turner *et al.* 1992) or partial melting of specific crustal protoliths, such as granulitic rocks from which a granitic melt was previously extracted (e.g., Collins *et al.* 1982) or charnockitic rocks which represent non-melt depleted, anhydrous granulitic protoliths (e.g., Jiang *et al.* 2009).

5.4 *Tectonic setting and implications for granitic magmatism*

The Late Jurassic Lengshuikeng granite porphyries and rhyolitic tuffs belong to calc-alkaline series and, with their low Ta and Yb contents, they plot within the field of volcanic arc granite in the Y *vs.* Nb and Yb *vs.* Ta diagrams (figure 9). These suggest that the Lengshuikeng district was situated in a continental arc environment during the Late Jurassic. In contrast, the Early Cretaceous Lengshuikeng syenogranites are somewhat alkalic and they plot in the field of within-plate granite

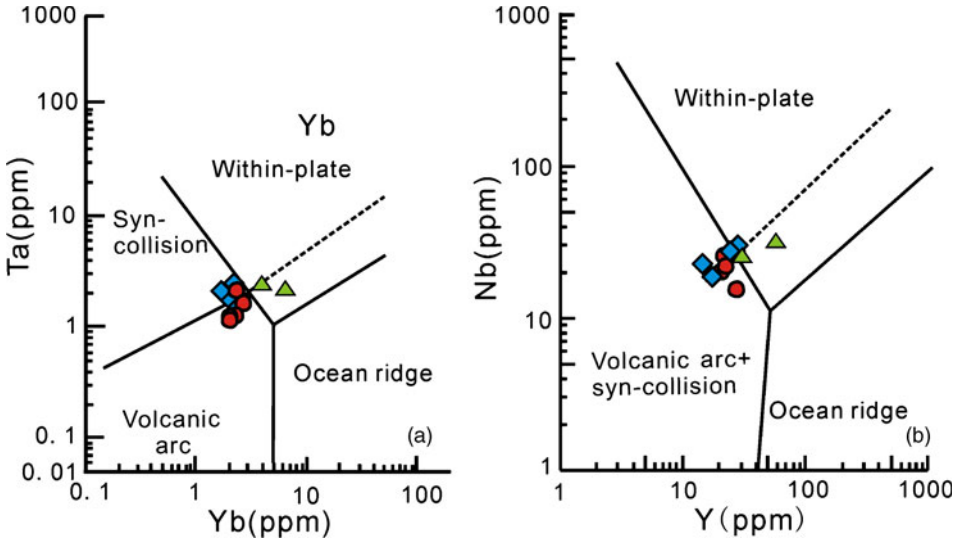

Figure 9. (**a**) Y *vs.* Nb (after Pearce *et al.* 1984) and (**b**) Yb *vs.* Ta. Symbols are as in figure 6. Data are from table 2.

in the Y *vs.* Nb and Yb *vs.* Ta diagrams (figure 9). The Palaeo-Pacific plate subduction zone is the only plate boundary present in this region during the late Mesozoic times (~161–155 Ma; figure 10a). The likely origin of the Early Cretaceous A-type syenogranites in this region as discussed above further suggests that back-arc extension has developed or an intra-arc rift has been formed since ~138 Ma (figure 10b).

Previous research has attempted to explain the ultimate tectonic cause of granitic magmatism in the southern Hunan to northern Guangxi region of SE China. There is a general consensus that Cretaceous (late Yanshanian) magmatism in SE China occurred in an active continental margin due to the subduction of the Palaeo-Pacific oceanic plate. However, the tectonic regime accounting for the more interior Jurassic (early Yanshanian) magmatism is controversial (Zhou and Li 2000; Li and Li 2007; Chen *et al.* 2008). Various tectonic scenarios include low-angle subduction models (Charvet *et al.* 2010; Jiang *et al.* 2011), an intracontinental orogen with post-orogenic extension (Hou and Yang 2009), an extensional basin-and-ranges province model (Gilder *et al.* 1991), and related models for intraplate rifting (Chen 1999; Li 2000; Xie *et al.* 2006). Despite some controversy, most researchers now consider that any of these scenarios could be related to the subduction of the Palaeo-Pacific plate (e.g., Martin *et al.* 1994; Lapierre *et al.* 1997; Zhou *et al.* 2012).

As mentioned earlier, the Indosinian collision between the South China and North China blocks began in the Late Palaeozoic and was over in the Late Triassic (ca. 270–208 Ma). As a response to the collision-orogeny between the South China and North China blocks, most areas of the Wuyi Mountains had been folded-uplifted and then extended-collapsed (Yu *et al.* 2009, 2010; Xu *et al.* 2010). The Yanshanian orogen began near the Late Triassic. During the early Yanshanian, there was a magmatic gap from 208 to 180 Ma in the South China Block. After that period of subdued igneous activity, magmatic activity began at ~185 Ma, but

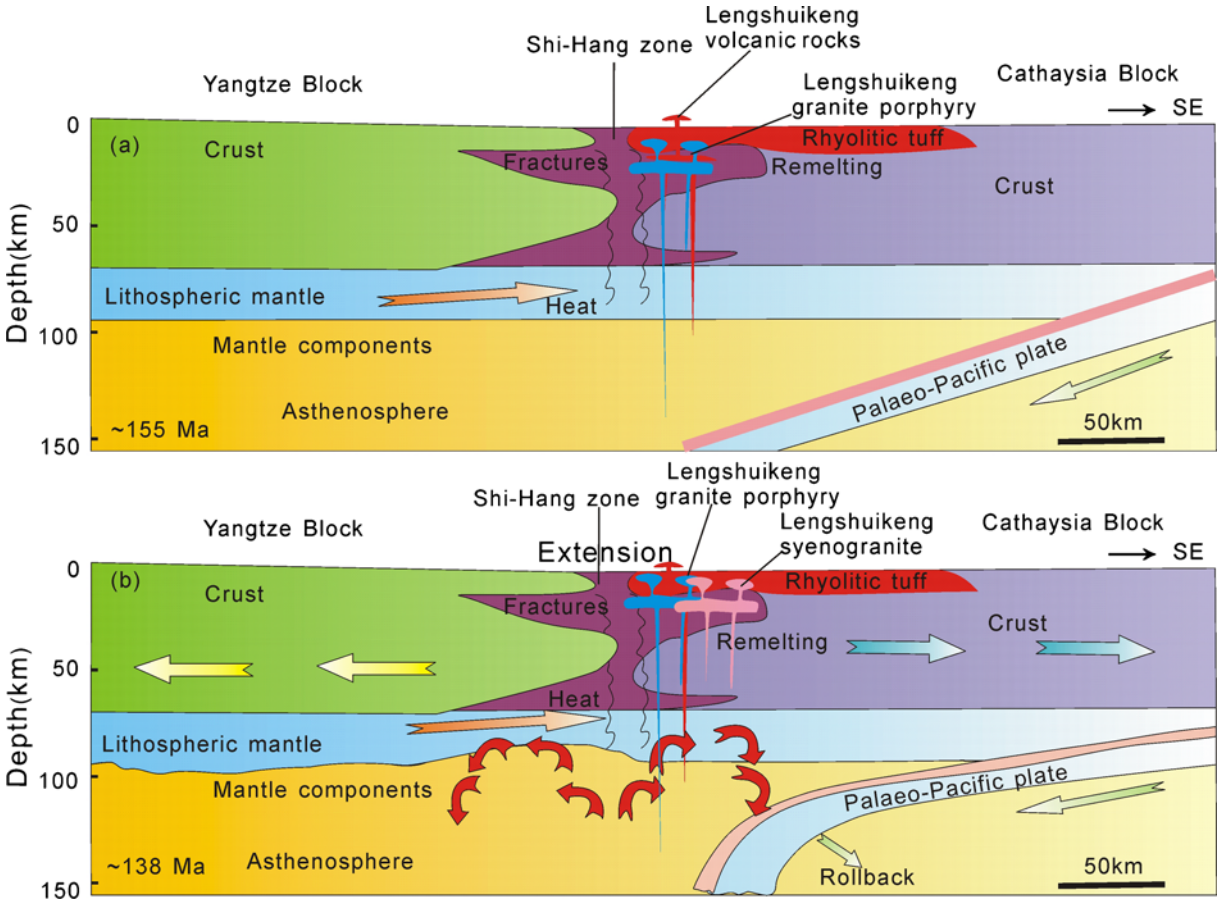

Figure 10. Tectonic models for the generation of the Lengshuikeng granite porphyries and syenogranites (modified after Jiang *et al.* 2009; Shu *et al.* 2009). (**a**) Middle Jurassic (~155 Ma), continental arc setting. The Palaeo-Pacific plate was subducted underneath the SCB at a very low angle. Partial melting with subsequent melts interacting with lithospheric mantle wedge formed the magma of the Lengshuikeng granite porphyries in a continental arc environment. (**b**) Since the Early Cretaceous (~138 Ma), a back-arc extension or intra-arc rift has been initiated as a consequence of slab roll-back of the Palaeo-Pacific plate. With ongoing extension and upwelling of asthenosphere, A-type syenogranites were formed.

main magmatic activities occurred mostly between ~180 and 170 Ma, such as bimodal magmatism in southeastern Hunan Province, A-type granitic magmatism in southern Jiangxi Province, and the mafic units (Zhao *et al.* 1998; Xie *et al.* 2006; Li *et al.* 2007). Since the Middle Jurassic, possibly from ~170 to ~155 Ma, the Palaeo-Pacific plate was subducted underneath the Chinese continent, and resulted in the formation of NE-trending compressive upwelling granites and thrust nappe structures (Chen 1999), i.e., especially in the Dexing ore field and the Lengshuikeng ore district (Deng *et al.* 2004; Hou and Yang 2009; Wang *et al.* 2011). Our new zircon U–Pb age data for the Lengshuikeng granite porphyries and rhyolitic tuff support the hypothesis that the Palaeo-Pacific plate was subducting underneath the Chinese continent at ca. 155 Ma ago (figure 10a). However, the palaeo-Pacific plate did not subduct successively towards the northwest but instead slab roll-back occurred since the beginning of Late Jurassic time (Jiang *et al.* 2009; Liu *et al.* 2010), which possibly lasted until Early Cretaceous (~138 Ma). This was followed by the formation of an intra-arc rift along the Shihang–Hang zone (Sun *et al.* 2005; Dong *et al.* 2007; Collins and Richards 2008). Subsequently, lithosphere extension, possibly accompanied by asthenosphere upwelling, may have triggered partial melting of the asthenosphere mantle. Injection of anomalously high temperature magma (derived by partial melting of asthenosphere mantle) into the crustal regions may have induced crustal rocks to melt partially, generating A-type magmas such as the Lengshuikeng syenogranites. Therefore, it is likely that the southern Hunan to northern Guangxi region is part of an intra-arc rift or back-arc extensional zone induced by subduction of Palaeo-Pacific plate (Hu *et al.* 2010; Xu *et al.* 2010; Yang *et al.* 2010). The likely formation and mixing of mantle- and crust-derived magmas induced by the crustal extension is the likely cause of granitic rocks in this region of SE China.

6. Conclusions

- Rhyolitic tuffs, granite porphyries and syenogranites in the Lengshuikeng ore district of SE China yielded zircon U–Pb ages of 161, 155 and 138 Ma, respectively.
- The Late Jurassic granite porphyries and rhyolitic tuffs in the Lengshuikeng ore district belong to calc-alkaline series, but exhibit geochemical characteristics of fractionated I-type granites. The Early Cretaceous syenogranites in the Lengshuikeng ore district are alkali-rich and show geochemical characteristics of A-type granites. However, the Lengshuikeng rhyolitic tuffs, granite porphyries and syenogranites were likely derived from the same magma sources, which were formed by partial melting of underlying Proterozoic meta-sedimentary rocks with minor addition of mantle-derived magmas, accompanied by fractional crystallization.
- Detailed petrologic and geochemical data for the Late Jurassic granite porphyries and rhyolitic tuffs in the Lengshuikeng ore district suggest that

  (a) during the Late Jurassic time, SE China on the southeast of the Shi-Hang zone was a continental arc associated with the subduction of the Palaeo-Pacific plate and
  (b) since the beginning of the Early Cretaceous an intra-arc rift has been formed along the Shi-Hang zone.

Acknowledgements

This research is jointly supported by China Bureau of Geological Survey project (Nos. 1212011085472, 1212010533105, 1212010981048), National Basic Research Program (No. 2009CB421008), Fundamental Research Funds for the Central Universities (No. 2010ZY02), State Key Laboratory of Geological Processes and Mineral Resources (No. GPMR201019), and the 111 Project (No. B07011). The authors would like to thank staff members of the China University of Geosciences (Beijing) for constructive discussions and comments.

References

Bea F, Pereira M D and Stroh A 1994 Mineral/leucosome trace-element partitioning in a peraluminous migmatite (a laser ablation-ICP-MS study); *Chem. Geol.* **117** 291–312.

Belousova E A, Suzanne G W and Fisher Y 2002 Igneous zircon: Trace element composition as an indicator of source rock type; *Contrib. Mineral. Petrol.* **143** 602–622.

Chappell B W and Stephens W E 1988 Origin of infracrustal (I-type) granite magmas; *Trans. Roy. Soc. Edinburgh-Earth Sci.* **79** 71–86.

Chappell B W and White A J R 1974 Two contrasting granite types; *Pacific Geology* **8** 173–174.

Charvet J, Lapierre H and Yu Y 1994a Geodynamic significance of the Mesozoic volcanism of southeastern China; *J. S. A. Earth Sci.* **68** 387–396.

Charvet J, Lapierre H and Yu Y W 1994b Geodynamic significance of the Mesozoic volcanism of southeastern China; *J. S. A. Earth Sci.* **9** 387–396.

Charvet J, Shu L S, Faure M, Choulet F, Wang B, Lu H F and Breton N L 2010 Structural development of the Lower Paleozoic belt of South China: Genesis of an intra-continental orogen; *J. Asian Earth Sci.* **39** 309–330.

Chen A 1999 Mirror-image thrusting in the South China orogenic belt: Tectonic evidence from western Fujian, southeastern China; *Tectonophys.* **305** 497–519.

Chen W and Zhou J P 1988 Mineralization of the Lengshuikeng porphyritic Ag–Pb–Zn deposit in Jiangxi Province; *J. Mineral. Petrol.* **8** 84–91 (in Chinese with English *abstract*).

Chen F R and Qiu Y Z 1995 Fluid geochemical modeling of ore-forming process of Lengshuikeng Ag, Pb, Zn porphyry deposit, Jiangxi, China and its geological implications; *Geochimica* **24** 24–32 (in Chinese with English *abstract*).

Chen J, Foland K, Xing F, Xu X and Zhou T 1991 Magmatism along the southeast margin of the Yangtze Block: Precambrian collision of the Yangtze and Cathaysia Blocks of China; *Geology* **19** 815–818.

Chen Z H, Wang D H, Qu W J, Chen Y C, Wang P A, Xu J X, Zhang J J and Xu M L 2006 Geological characteristics and mineralization age of Taoxikeng tungsten deposit in Chongyi County, southern Jiangxi Province, China; *Geol. Bull. China* **25** 495–501 (in Chinese with English *abstract*).

Chen C H, Lee C Y and Shinjo R 2008 Was there Jurassic Paleo-Pacific subduction in South China?: Constraints from $^{40}Ar/^{39}Ar$ dating, elemental and Sr–Nd–Pb isotopic geochemistry of the Mesozoic basalts; *Lithos* **106** 83–92.

Chen Z H, Guo K Y, Dong Y G, Chen R G, Li L M, Liang Y H, Li C H, Yu X M, Zhao L and Xing G F 2009 Possible early Neoproterozoic magmatism associated with slab window in the Pingshui segment of the Jiangshan–Shaoxing suture zone: Evidence from zircon LA-ICP-MS U–Pb geochronology and geochemistry; *Sci. China Ser.* **D52** 925–939.

Clemens J D 2003 S-type granitic magmas – petrogenetic issues, models and evidence; *Earth Sci. Rev.* **61** 1–18.

Collins W J and Richards S W 2008 Geodynamic significance of S-type granites in circum-Pacific orogens; *Geology* **36** 559–562.

Collins W J, Beams S D and White A J R 1982 Nature and origin of A-type granites with particular reference to southeastern Australia; *Contrib. Mineral. Petrol.* **80** 189–200.

Creaser R A, Price R C and Wormald R J 1991 A-type granites revisited: Assessment of a residual source model; *Geology* **19** 163–166.

Deng S M 1991 Cryptoexplosive breccia dyke in the paleovolcanic rock zone in Lengshuikeng, Guixi, Jiangxi Province and its metallogeny; *Geol. Sci. Technol. Jiangxi* **18** 28–32 (in Chinese with English *abstract*).

Deng J F, Luo Z H and Su S G 2004 *Lithogenesis, tectonic setting and metallogeny*; Geological Publishing House, Beijing, 381p. (in Chinese).

Deng J, Wang Q F, Yang S J, Liu X F, Zhang Q Z, Yang L Q and Yang Y H 2009a Self-similar fractal analysis of gold mineralization of Dayingezhuang disseminated-veinlet deposit in Jiaodong gold province, China; *J. Geochem. Explor.* **102** 95–102.

Deng J, Yang L Q, Gao B F, Sun Z S, Guo C Y, Wang Q F and Wang J P 2009b Fluid evolution and metallogenic dynamics during tectonic regime transition: Example from the Jiapigou gold belt in Northeast China; *Resour. Geol.* **59** 140–152.

Deng J, Wang Q F, Yang S J, Liu X F, Zhang Q Z, Yang L Q and Yang Y H 2010 Genetic relationship between the E'meishan plume and the bauxite deposits in Western Guangxi, China: Constraints from U–Pb and Lu–Hf isotopes of the detrital zircons in bauxite ores; *J. Asian Earth Sci.* **37** 412–424.

Deng J, Wang Q F, Xiao C H, Yang L Q, Liu H, Gong Q J and Zhang J 2011a Tectonic–magmatic–metallogenic system, Tongling ore cluster region, Anhui Province, China; *Inter. Geol. Rev.* **53** 449–476.

Deng J, Wang Q F, Wan L, Liu H, Yang L Q and Zhang J 2011b A multifractal analysis of mineralization characteristics of the Dayingezhuang disseminated-veinlet gold deposit in the Jiaodong gold province of China; *Ore Geol. Rev.* **53** 54–64.

Deng J, Yang L Q and Wang C M 2011c Research advance of superimposed orogenesis and metallogenesis in the Sanjiang Tethys; *Acta Petrol. Sinica* **27** 2501–2509 (in Chinese with English *abstract*).

Dong S W, Zhang Y Q, Long C X, Liu Z Y, Ji Q, Wang T, Hu J M and Chen X H 2007 Jurassic tectonic revolution in China and new interpretation of the Yanshan movement; *Acta Geol. Sinica* **81** 1449–1461 (in Chinese with English *abstract*).

Dostal J and Chatterjee A K 2000 Contrasting behaviour of Nb/Ta and Zr/Hf ratios in a peraluminous granitic pluton (Nova Scotia, Canada); *Chem. Geol.* **163** 207–218.

Eby G N 1992 Chemical subdivision of the A-type granitoids: petrogenetic and tectonic implications; *Geology* **20** 641–644.

Ewart A and Griffin W L 1994 Application of proton-microprobe data to trace-element partitioning in volcanic rocks; *Chem. Geol.* **117** 251–284.

Faure G 1986 *Principles of Isotope Geology*; John Wiley & Sons, Chichester, 589p.

Frost B R, Arculus R J, Barnes C G, Collins W J, Ellis D J and Frost C D 2001 A geochemical classification of granitic rocks; *J. Petrol.* **42** 2033–2048.

Frost C D, Frost B R, Bell J M and Chamberlain K R 2002 The relationship between A-type granites and residual magmas from anorthosite: Evidence from the northern Sherman batholith, Laramie Mountains, Wyoming, USA; *Precamb. Res.* **119** 45–71.

Gehrels G E, Valencia V and Pullen A 2006 Detrital zircon geochronology by Laser-Ablation Multicollector ICPMS at the Arizona Laser Chron Center; In: *Geochronology: Emerging Opportunities*, Paleontology Society Short Course (eds) Loszewski T and Huff W; Paleontology Society Papers, pp. 1–10.

Gilder S A, Keller G R, Luo M and Goode P C 1991 Eastern Asia and the western Pacific timing and spatial distribution of rifting in China; *Tectonophys.* **197** 225–243.

Hickmott D D, Sorensen S S and Rogers P S Z 1992 Metasomatism in a subduction complex: Constraints from microanalysis of trace elements in minerals from garnet amphibolite from the Catalina Schist; *Geology* **20** 347–350.

Hoskin P W O and Black L P 2000 Metamorphic zircon formation by solid-state recrystallization of protolith igneous zircon; *J. Metamorph. Geol.* **18** 423–439.

Hou Z and Yang Z 2009 Porphyry deposits in continental settings of China: Geological characteristics, magmatic-hydrothermal system, and metallogenic model; *Acta Geol. Sinica* **83** 1781–1817.

Hsieh P S, Chen C H, Yang H J and Lee C Y 2008 Petrogenesis of the Nanling Mountains granites from South China: Constraints from systematic apatite geochemistry and whole-rock geochemical and Sr–Nd isotope compositions; *J. Asian Earth Sci.* **33** 428–451.

Hsü K J, Li J L, Chen H H, Wang Q C, Sun S and Sengör A M C 1990 Tectonics of South China: Key to understanding West Pacific geology; *Tectonophys.* **183** 9–39.

Hu R Z, Mao J W, Fan W M, Hua R M, Bi X W, Zhong H, Song X Y and Tao Y 2010 Some scientific questions on the intra-continental metallogeny in the South China continent; *Earth Sci. Frontiers* **17** 13–26 (in Chinese with English *abstract*).

Jahn B M, Chen P Y and Yen T P 1976 Rb–Sr ages of granitic rocks in southeastern China and their tectonic significance; *Geol. Soc. Am. Bull.* **86** 763–766.

Jahn B M, Zhou X H and Li J L 1990 Formation and tectonic evolution of southeastern China and Taiwan: Isotopic and geochemical constraints; *Tectonophys.* **183** 145–160.

Jahn B M, Wu F Y, Capdevila R, Martineau F, Zhao Z H and Wang Y X 2001 Highly evolved juvenile granites with tetrad REE patterns: The Woduhe and Baerzhe granites from the Great Xing'an Mountains in NE China; *Lithos* **59** 171–198.

Jiang Y H, Jiang S Y, Dai B Z, Liao S Y, Zhao K D and Ling H F 2009 Middle to Late Jurrasic felsic and mafic magmatism in southern Hunan province, southeast China: Implications for a continental arc to rifting; *Lithos* **107** 185–204.

Jiang Y H, Zhao P, Zhou Q, Liao S Y and Jin G D 2011 Petrogenesis and tectonic implications of Early Cretaceous S and A-type granites in the northwest of the Gan-Hang rift, SE China; *Lithos* **121** 55–73.

Jiangxi Bureau of Geology and Mineral Exploration and Development (JBGMED) 1982 *Geological history of Jiangxi Province*; Geological Publishing House, Beijing, 120p. (in Chinese).

Lan C Y, Jahn B M, Mertzman S A and Wu T W 1996 Subduction-related granitic rocks of Taiwan; *J. S. A. Earth Sci.* **14** 11–28.

Lapierre H, Jahn B M, Charvet J and Cddex R 1997 Mesozoic felsic arc magmatism and continental olivine tholeiites in Zhejiang Province and their relationship with the tectonic activity in southeastern China; *Tectonophys.* **274** 321–338.

Li L M, Sun M, Wang Y J, Zhao G C, Lin S F, Xi X P, Chan L S, Zhang F F and Wong J 2011 U–Pb and Hf isotopic study of zircons from migmatised amphibolites in the Cathaysia Block: Implications for the early Paleozoic peak tectonothermal event in southeastern China; *Gondwana Res.* **19** 191–201.

Li X H 2000 Cretaceous magmatism and lithospheric extension in southeast China; *J. Asian Earth Sci.* **18** 293–305.

Li X H, Li Z X, Li W X, Liu Y, Yuan C, Wei G G and Qi C S 2007 U–Pb zircon, geochemical and Sr–Nd–Hf isotopic constraints on age and origin of Jurassic I and A-type granites from central Guangdong, SE China: A major igneous event in respond to foundering of a subducted flat-slab?; *Lithos* **96** 186–204.

Li X H, Li W X, Li Z X and Liu Y 2008 850–790 Ma bimodal volcanic and intrusive rocks in northern Zhejiang, South China: A major episode of continental rift magmatism during the breakup of Rodinia; *Lithos* **102** 341–357.

Li Z X, Zhang L and Powell C M 1996 Positions of the East Asian cratons in the Neoproterozoic supercontinent Rodinia; *Aust. J. Earth Sci.* **43** 593–604.

Li Z X and Li X H 2007 Formation of the 1300 km-wide intracontinental orogen and post-orogenic magmatic province in Mesozoic South China: A flat-slab subduction model; *Geology* **35** 179–182.

Linnen R L and Keppler H 1997 Columbite solubility in granitic melts: Consequences for the enrichment and fractionation of Nb and Ta in the Earth's crust; *Contrib. Mineral. Petrol.* **128** 213–227.

Liu J Y 1985 Xiangshan igneous pluton – a granitic hypabyssal intrusive volcanic complex; *Geochimica* **2** 142–149 (in Chinese with English *abstract*).

Liu J, Ye H S, Xie G Q, Yang G Q and Zhang W 2008 Re–Os dating of molybdenite from the Hukeng tungsten deposit in the Wugongshan area, Jiangxi Province, and its geological implications; *Acta Geol. Sinica* **82** 1576–1584 (in Chinese with English *abstract*).

Liu R, Zhou H W, Zhong Z Q, Zhong Z Q, Zeng W, Xiang H, Jin S, Lu X Q and Li C Z 2010 Zircon U–Pb ages and Hf isotope compositions of the Mayuan migmatite complex, NW Fujian Province, southeast China: Constraints on the timing and nature of a regional tectonothermal event associated with the Caledonian orogeny; *Lithos* **119** 163–180.

Liu X and Shen S L 1991 Some problems of tectonogeochemistry in Lengshuikeng Ag–Pb–Zn ore field, Jiangxi province, China; *Geotectonica et Metallogenia* **15** 41–54 (in Chinese with English *abstract*).

Loiselle M C and Wones D R 1979 Characteristics and origin of anorogenic granites; *Geol. Soc. Am. Abstracts with Programs* **11** 468.

Luo Z J 1991 Wall rock alternation of the porphyritic Ag–Pb–Zn deposit in Lengshuikeng; *Geol. Jiangxi* **5** 3–10 (in Chinese with English *abstract*).

Mao J W, Zhang Z H, Yu J J, Wang Y T and Niu B G 2003 Geodynamic settings of Mesozoic large-scale mineralization in the North China and adjacent areas: Implication from the highly precise and accurate ages of metal deposits; *Sci. China Ser.* **D33** 289–299 (in Chinese with English *abstract*).

Martin H, Bonin B, Capdevila R, Jahn B M, Lameyre J and Wang Y 1994 The Kuiqi peralkaline granitic complex (SE China): Petrology and geochemistry; *J. Petrol.* **35** 983–1015.

Mckee E H, Rytuba J J and Xu K 1987 Geochronology of Xihuashan composite granitic body and tungsten mineralization, Jiangxi Province, South China; *Econ. Geol.* **82** 218–223.

Meng X J, Dong G Y and Liu J G 2007 *Lengshuikeng porphyry Pb–Zn–Ag deposit in Jiangxi Province*; Geological Publishing House, Beijing, 184p. (in Chinese).

Meng X J, Hou Z Q, Dong G Y, Liu J G, Zuo L Y and Yang Z S 2009 Geological characteristics and mineralization timing of the Lengshuikeng porphyry Pb–Zn–Ag deposit, Jiangxi Province; *Acta Geol. Sinica* **83** 1951–1967 (in Chinese with English *abstract*).

Miller C F 1995 Are strongly peraluminous magmas derived from pelitic sedimentary sources; *J. Geol.* **93** 673–689.

No. 912 Geological Surveying Team (NGST) 1997 *Geology report on the Lengshuikeng Ag deposit, Guixi County, Jiangxi Province*; Jiangxi Bureau of Geology and Mineral Exploration and Development, Nanchang, 53p. (in Chinese).

No. 912 Geological Surveying Team (NGST) 2003 *Geology report on the Lengshuikeng Ag deposit, Guixi County, Jiangxi Province*; Jiangxi Bureau of Geology and Mineral Exploration and Development, Nanchang, 109p. (in Chinese).

Pan Y M and Dong P 1999 The lower Changjiang (Yangzi/Yangtze River) metallogenic belt, east central China: Intrusion and wall rock-hosted Cu–Fe–Au, Mo, Zn, Pb, Ag deposits; *Ore Geol. Rev.* **15** 177–241.

Pearce J A, Harris N B W and Tindle A G 1984 Trace element discrimination diagrams for the tectonic interpretation of granitic rocks; *J. Petrol.* **25** 956–983.

Raharimahefa T and Kusky T M 2010 Temporal evolution of the Angavo and related shear zones in Gondwana: Constraints from LA-MC-ICP-MS U–Pb zircon ages of granitoids and gneiss from central Madagascar; *Precamb. Res.* **182** 30–42.

Rapp R P and Watson E B 1995 Dehydration melting of metabasalt at 8–32 kbar: Implications for continental growth and crust–mantle recycling; *J. Petrol.* **36** 891–931.

Shu L S and Charvet J 1996 Kinematic and geochronology of the Proterozoic Dongxiang–Shexian ductile shear zone (Jiangnan region, South China); *Tectonophys.* **267** 291–302.

Shu L S, Faure M, Jiang S Y, Yang Q and Wang Y J 2006 SHRIMP zircon U–Pb age, litho- and biostratigraphic analyses of the Huaiyu Domain in south China – evidence for a Neoproterozoic orogen, not Late Paleozoic–Early Mesozoic collision; *Episodes* **29** 244–252.

Shu L S, Zhou G Q, Shi Y S and Yin J 1994 Study of the high pressure metamorphic blueschist and its Neoproterozoic age in the Eastern Jiangnan belt; *Chinese Sci. Bull.* **39** 1200–1204.

Shu L S, Zhou X M, Deng P, Wang B, Jiang S Y, Yu J H and Zhao X X 2009 Mesozoic tectonic evolution of the southeast China Block: New insights from basin analysis; *J. Asian Earth Sci.* **34** 376–391.

Smith R E and Smith S E 1976 Comments on the use of Ti, Zr, Y, Sr, K, P and Na in classification of basaltic magmas; *Earth Planet. Sci. Lett.* **32** 114–120.

Stacey J S and Kramers J D 1975 Approximation of terrestrial lead isotope evolution by a two-stage model; *Earth Planet. Sci. Lett.* **26** 207–221.

Sun S S and McDonough W F 1989 Chemical and isotopic systematics of oceanic basalts: Implications for mantle composition and processes; In: *Magmatism in the Ocean Basin* (eds) Sunders A D and Norry M J, *Geol. Soc. London Spec. Publ.*, pp. 313–345.

Sun T, Zhou X M and Chen P R 2005 The genesis and significance of Mesozoic strong aluminum granites in eastern Nanling; *Sci. China Ser.* **D48** 165–174.

Sylvester P J 1998 Post-collisional strongly peraluminous granites; *Lithos* **45** 29–44.

Turner S P, Foden J D and Morrison R S 1992 Derivation of some A-type magmas by fractionation of basaltic magma: An example from the Padthaway Ridge, South Australia; *Lithos* **28** 151–179.

Wang Y, Guan T Y, Huang G F, Yu D and Chen C 2002 Isotope chronological studies of late Yanshanian volcanic rocks in northeast Jiangxi Province; *Acta Geosci. Sinica* **23** 233–236 (in Chinese with English *abstract*).

Wang Y J, Fan W M, Zhao G C, Ji S C and Peng T P 2007 Zircon U–Pb geochronology of gneissic rocks in the Yunkai massif and its implications on the Caledonian event in the south China Block; *Gondwana Res.* **12** 404–416.

Wang C M, Cheng Q M, Zhang S T, Deng J and Xie S Y 2008 Magmatic hydrothermal superlarge systems – a case study of the Nannihu ore field; *J. China University Geosci.* **19** 391–403.

Wang C M, Deng J, Zhang S T and Yang L Q 2010a Metallogenic province and large scale mineralization of VMS deposits in China; *Resour. Geol.* **60** 404–413.

Wang C M, Deng J, Zhang S T, Xue C J, Yang L Q, Wang Q F and Sun X 2010b Sediment-hosted Pb–Zn deposits in Southwest Sanjiang Tethys and Kangdian area on the western margin of Yangtze Craton; *Acta Geol. Sinica* **84** 1428–1438.

Wang C M, Wu G G, Zhang D, Luo P, Di Y J and Yu X Q 2010c The regional metallogeny and mineralizing pedigree of northeastern Jiangxi regain, China; *Global Geol.* **29** 588–600 (in Chinese with English *abstract*).

Wang C M, Xu Y G, Wu G G, Zhang D, Yang L, Liu J G, Wan H Z, Di Y J, Yu X Q and Zhang Y Y 2011 C, O, S and Pb isotopes and sources of the ore metals of the Lengshuikeng Ag–Pb–Zn ore field, Jiangxi; *Earth Sci. Frontiers* **18** 179–193 (in Chinese with English *abstract*).

Wei M X 1997 Relationship between alternated carbonate minerals and silver mineralization in the Lengshuikeng porphyry silver deposit, Jiangxi; *Miner. Resour. Geol.* **1** 39–45 (in Chinese with English *abstract*).

Whalen J B, Currie K L and Chappell B W 1987 A-type granites: Geochemical characteristics, discrimination and petrogenesis; *Contrib. Mineral. Petrol.* **95** 407–419.

Winchester J A and Floyd P A 1977 Geochemical discrimination of different magma series and their differentiation products using immobile elements; *Chem. Geol.* **20** 325–343.

Wong J, Sun M, Xing G F, Zhao G C, Wong K and Wu F Y 2011 Zircon U–Pb and Hf isotopic study of Mesozoic felsic rocks from eastern Zhejiang, south China: Geochemical contrast between the Yangtze and Cathaysia blocks; *Gondwana Res.* **19** 244–259.

Wu F Y, Jahn B M, Wilder S A, Lo C H, Yui T F, Lin Q L, Ge W C and Sun D Y 2003 Highly fractionated I-type granites in NE China (I): Geochronology and petrogenesis; *Lithos* **66** 241–273.

Xie X, Xu X S, Zou H B, Jiang S Y, Zhang M and Qiu J S 2006 Early J2 basalts in SE China: Incipience of large-scale late Mesozoic magmatism; *Sci. China Ser.* **D49** 796–815.

Xiong X L, Adam J and Green T H 2005 Rutile stability and rutile/melt HFSE partitioning during partial melting of hydrous basalt: Implications for TTG genesis; *Chem. Geol.* **218** 339–359.

Xu W X, Xiao M H and Chen M Y 2001 Stable isotope characteristics of minerals in the Lengshuikeng porphyry Ag–Pb–Zn deposit in Jiangxi Province; *Bull. Mineral. Petrol. Geochem.* **20** 370–372 (in Chinese with English *abstract*).

Xu X B, Zhang Y Q, Shu L S, Wang R R and Xu H Z 2010 Geochronology of zircon LA-ICP-MS U–Pb and muscovite $^{40}Ar/^{39}Ar$: Constrains to Early Yanshanian event in southeast China; *Geol. Sci. Technol. Infor.* **29** 87–93 (in Chinese with English *abstract*).

Yang M G and Luo X 1998 *Metallogenetic Regularity and Prognosis of Wuyi Uplift and Chenzhou–Shangrao Depression*; Geological Publishing House, Beijing, 21p. (in Chinese).

Yang S Y, Jiang S Y, Jiang Y H, Jiang S D and Fan H H 2010 Zircon U–Pb geochronology, Hf isotopic composition and geological implications of the rhyodacite and rhyodacitic porphyry in the Xiangshan uranium ore field, Jiangxi Province, China; *Sci. China Ser.* **D40** 953–969 (in Chinese with English *abstract*).

Yao J 2003 Geological characteristic of ore body of the Yinluling mine and some new recognitions yield from the geologic work; *Nonferrous Metals* **55** 11–12 (in Chinese with English *abstract*).

Ye Q T 1987 *Metallogenetic Series and Mechanism of Lead–zinc Ore Deposits in Northeast Jiangxi*; Beijing Science and Technology Press Publishing House, Beijing, 114p. (in Chinese).

Yin J W, Kim S J, Lee H K and Itaya T 2002 K–Ar ages of plutonism and mineralization at the Shizhuyuan W–Sn–Bi–Mo deposit, Hunan Province, China; *J. Asian Earth Sci.* **20** 151–155.

Yu X Q, Di Y J, Wu G G, Zhang D, Zheng Y and Dai Y P 2009 The Early Jurassic magmatism in northern Guangdong Province, southeastern China: Constraints from SHRIMP zircon U–Pb dating of Xialan complex; *Sci. China Ser.* **D52** 471–483.

Yu X Q, Wu G G, Zhang D, Yan T Z, Di Y J and Wang L W 2006 Cretaceous extension of the Ganhang Tectonic Belt, southeastern China: Constraints from geochemistry of volcanic rocks; *Cretaceous Res.* **27** 663–672.

Yu X Q, Wu G G, Zhao X X, Gao J F, Di Y J, Zheng Y, Dai Y P, Li C L and Qiu J T 2010 The Early Jurassic tectono-magmatic events in southern Jiangxi and northern Guangdong provinces, SE China: Constraints from the SHRIMP zircon U–Pb dating; *J. Asian Earth Sci.* **39** 408–422.

Yu Y W, Xu B T, Chen J F and Dong C W 2001 Nd isotopic systematics of the Cretaceous volcanic rocks from southeastern Zhejiang Province, China: Implications for stratigraphic study; *Geol. J. China Universities* **7** 62–69 (in Chinese with English *abstract*).

Yuan Z X and Wu L S 1991 The Sm–Nd, Rb–Sr isotopic age-dating of Mayuan group in Northern Fujian; *Acta Petrol. Mineral* **10** 127–132 (in Chinese with English *abstract*).

Zhang J J, Chen Z H, Wang D H, Chen Z Y, Liu S B and Wang C H 2008 Geological characteristics and metallogenic epoch of the Xinlekeng tungsten deposit; *Geotectonica et Metallogenia* **32** 92–97 (in Chinese with English *abstract*).

Zhang J J, Wu M S, Chen Z H, Liu S B, Li L X, Qiu L M, Wu B, Huang A and Zhu P J 2009 Geochronologic study on the Jinzhuping molybdenum-polymetallic deposit from Shangrao of Jiangxi Province; *Rock and Mineral Analysis* **28** 228–232 (in Chinese with English *abstract*).

Zhao Z H, Bao Z W and Zhang B Y 1998 Geochemical features of Mesozoic basalts in South Hunan; *Sci. China Ser.* **D28** 102–112 (in Chinese).

Zhou J X 1999 *Geochemistry and Petrogenesis of Igneous Rocks Containing Amphibole and Mica: A Case Study of Plate Collision Involving Scotland and Himalayas* (New York and Beijing: Science Press), pp. 41–72.

Zhou M F, Yan D P, Kennedy A K, Li Y and Ding J 2002 SHRIMP U–Pb zircon geochronological and geochemical evidence for Neoproterozoic arc-magmatism along the western margin of the Yangtze block, south China; *Earth Planet. Sci. Lett.* **196** 51–67.

Zhou Q, Jiang Y H, Zhao P, Liao Y S and Jin G D 2012 Origin of the Dexing Cu-bearing porphyries, SE China: Elemental and Sr–Nd–Pb–Hf isotopic constraints; *Int. Geol. Rev.* **54** 572–592.

Zhou X M and Li X W 2000 Origin of Late Mesozoic rocks in southeastern China: Implications for lithosphere subduction and underplating of mafic magmas; *Tectonophys.* **326** 269–287.

Zuo L Y, Hou Z Q, Meng X J, Yang Z M, Yong Y C and Li Z 2010 SHRIMP U–Pb zircon geochronology of the ore-bearing rock in the Lengshuikeng porphyry type Ag–Pb–Zn deposit; *Geol. China* **37** 1450–1456 (in Chinese with English *abstract*).

Zuo L Y, Meng X J and Yang Z S 2008 Petrochemistry and Sr, Nd isotopes of intrusive in Lengshuikeng porphyry type Ag–Pb–Zn deposit; *Mineral Deposit* **27** 367–382 (in Chinese with English *abstract*).

MS received 19 July 2012; revised 27 November 2012; accepted 9 December 2012